Injury and Healing Effect on Fatigue Properties of Collagen V Haploinsufficient Female Murine Tendons

Carlson JA[1], Beach ZM[1], Weiss SN[1], Birk DE[2], Soslowsky LJ[1]
[1]McKay Orthopaedic Research Laboratory, University of Pennsylvania, Philadelphia, PA, [2] University of South Florida, Tampa, FL
Disclosures: Carlson JA(N), Beach ZM(N), Weiss SN(N), Birk DE(N), Soslowsky LJ(N)

INTRODUCTION: Patients with Classic Ehlers-Danlos Syndrome (*c*EDS), a disorder characterized by mutation in the *COL5* genes with *COL5a1* haploinsufficiency being the most common, suffer from articular hypermobility, skin hyperextensibility, tendon/ligament fragility and abnormal wound healing [1,2]. Furthermore, human studies have shown that females have decreased collagen synthesis and fibroblast activity [3,4] as well as altered gene expression during repair [5], potentially exacerbating detrimental changes present in *c*EDS tendons. Quasi-static loading of the mouse patellar tendon [6,7,8] demonstrates decreases in modulus, failure stress, failure load, and stiffness due to reduced collagen V throughout healing. Although the hierarchical structure of the tendon has been implicated in changes following cyclic fatigue loading, and collagen V is essential in regulating collagen fibrillogenesis, fatigue properties have not been examined in *c*EDS tendons [6,9]. Therefore, the objective of this study was to define the fatigue properties of female patellar tendons following injury, as well as the effect of a reduction in collagen V on these properties. We hypothesized that reduction in collagen V following injury will delay improvements in the fatigue properties compared to wild-type tendons.

METHODS: Adult female wild-type (WT) C57/BL6 and heterozygous ***Col5a1***$^{+/-}$ mice, a model for *c*EDS, at 120 days of age (n=60) were used (IACUC approved). Mice were randomly divided into uninjured and injured groups, with injured mice undergoing bilateral patellar tendon injury surgery as described [10]. Injured mice were sacrificed early in the remodeling healing phase (3w) or later in remodeling (6w) and uninjured age-matched mice were sacrificed. *Mechanics.* The patella-patellar tendon-tibia complexes of all mice were dissected and prepared for mechanical testing [11]. Cross-sectional area was measured using a custom laser device [12]. Tendons underwent a fatigue protocol, consisting of pre-conditioning and 1 Hz cyclic loading until failure. Cyclic loads corresponded to 20% and 55% maximum stress (previously determined from quasi-static testing). Fatigue parameters were analyzed at the end of the primary phase (BP1) and secondary phase (BP2) of fatigue life, capturing changes in material parameters that occur with fatigue damage, including peak cyclic strain, tangent modulus, secant modulus, tangent stiffness, secant stiffness, hysteresis, and laxity. Secant modulus and stiffness are calculated in reference to the zero displacement point and tangent modulus and stiffness are calculated from a specific loading cycle. *Statistics.* Two-way ANOVAs with post-hoc Bonferroni tests were used to assess the effects of genotype (collagen V expression), injury time-point, and their interaction on fatigue mechanical properties. Significance was set at $p \leq 0.05$ and trends at $p \leq 0.1$.

RESULTS: WT patellar tendons 3w post-injury (PI) showed a significant decrease in tangent modulus (BP1 and BP2) (Fig.1A,B), tangent stiffness (BP1 and BP2 [trend]) (Fig.1C,D), and secant modulus (BP1 and BP2) (not shown) when compared to uninjured controls. The decrease in tangent modulus at BP2 persisted to 6w PI. However, no other parameters had differences at 6w PI. ***Col5a1***$^{+/-}$ patellar tendons 3 and 6w PI exhibited reduced tangent modulus (Fig.1A,B), tangent stiffness (Fig.1C,D), and secant modulus at both BP1 and BP2 when compared to uninjured controls. There were no differences in ***Col5a1***$^{+/-}$ tendons compared to uninjured tendons in peak strain (Fig.2C) or secant stiffness (not shown) at BP1. However, 3w PI at BP2, there was an increase in peak strain (Fig.2D) and a trending decrease in secant stiffness (not shown), with no differences 6w PI. Hysteresis was significantly higher in WT tendons 3w PI when compared to uninjured and 6w tendons at BP1. However only a trending difference was seen at BP2 between uninjured and 3w PI (Fig.2A,B). ***Col5a1***$^{+/-}$ tendons showed no differences in hysteresis at BP1, but had significantly higher hysteresis 3 and 6w PI compared to uninjured tendons at BP2, and a trending increase between 3 and 6w PI (Fig.2A,B). Differences between genotypes, were primarily seen in the uninjured groups, with WT tendons having a significantly lower tangent modulus (BP1 and BP2) (Fig.1A,B), tangent stiffness (BP1) (Fig.1C), and secant modulus (BP1 and BP2) (not shown), and a significantly higher laxity (BP1) (not shown). When compared to WT tendons, ***Col5a1***$^{+/-}$ tendons at 6w PI had a decreased peak strain (BP2) (Fig.2D) and increased secant stiffness (BP1 [trend] and BP2) (not shown).

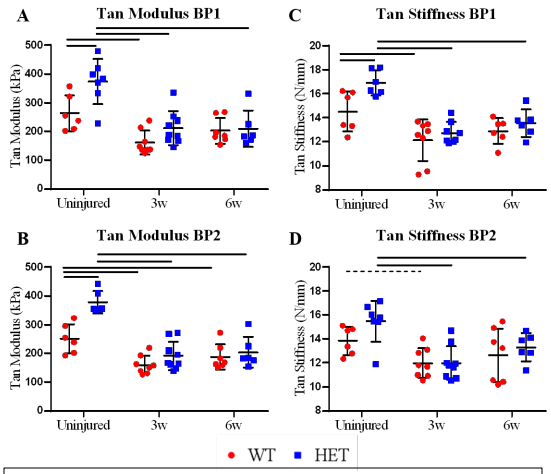

Figure 1: Tangent Modulus BP1 (A) and BP2 (B). Tangent Stiffness BP1 (C) and BP2 (D). ***Col5a1***$^{+/-}$ tendons had persistent decreases in tangent modulus and tangent stiffness 3 and 6w PI at BP1 and BP2. WT tendon decreases in tangent modulus and tangent stiffness seen 3w PI were only persistent to 6w PI in tangent modulus at BP2. Solid lines denote significance and dashed lines denote trends.

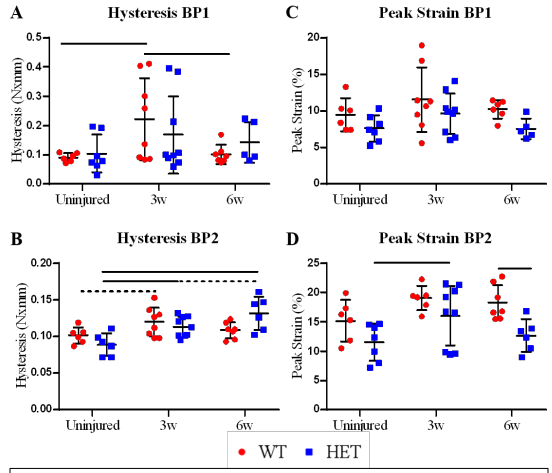

Figure 2: Hysteresis BP1 (A) and BP2 (B). WT tendons had increased hysteresis at BP1 3w PI, while ***Col5a1***$^{+/-}$ tendons had increased hysteresis 3 and 6w PI at BP2. **Peak Strain BP1 (C) and BP2 (D).** Peak strain was increased 3w PI in ***Col5a1***$^{+/-}$ tendons at BP2. Solid lines denote significance and dashed lines denote trends.

DISCUSSION: This study evaluated the fatigue properties of the patellar tendon in uninjured and injured mice as well as the role of collagen V. Cyclic fatigue loading mimics the *in vivo* loading pattern of the patellar tendon, and therefore is a relevant approach to study mechanic properties. Overall, fatigue properties of ***Col5a1***$^{+/-}$ tendons were persistently affected to a later time-point post-injury, while the fatigue properties of WT tendons showed minimal differences later in healing. Therefore, as hypothesized, collagen V deficient mice have a delayed healing response, with changes persisting to 6w PI, while WT tendon fatigue properties recover by 6w PI. Additionally, genotypic differences in uninjured tendons indicate that collagen V plays a role in the tendon response to cyclic loading. However, these differences are not consistently present PI. This shows that WT and ***Col5a1***$^{+/-}$ tendon fatigue properties are affected to different degrees following injury, and the diminished healing of ***Col5a1***$^{+/-}$ tendons could be obscuring genotypic differences post-injury. Lastly, hysteresis analysis indicates that energy loss is different throughout fatigue life between WT and ***Col5a1***$^{+/-}$ tendons following injury, as WT tendons show increased hysteresis at the end of the primary phase, while ***Col5a1***$^{+/-}$ tendons show increased hysteresis at the end of the secondary phase. More energy is lost at the end of fatigue life in ***Col5a1***$^{+/-}$ tendons, while the opposite is true for WT tendons. This indicates that collagen V affects the ability of the tendon to heal in a manner that resists microstructural damage associated with cyclic use. Therefore, this study demonstrates that collagen V plays a role in the tendon's ability to respond to fatigue loading, and following injury, collagen V plays a crucial role in the tendon healing process.

SIGNIFICANCE: This study demonstrates that WT tendon fatigue properties recover following injury while a decrease in collagen V results in a delayed healing response, highlighting the importance of evaluating the effect of collagen V in the tendon healing process.

REFERENCES: [1] Steinmann B et al. *Connective Tissue and Its Heritable Disorders.* Wiley-Liss; 2002. [2] Wenstrup RJ et al. *J Biol Chem.* 2006. [3] Ainsworth SR et al. *CORR.* 1993. [3] Yu WD et al. *CORR.* 2001. [4] Kjaer M et al. *J. Anat.* 2006. [5] Hart DA et al. *CORR.* 1998. [6] Johnston JM et al. *J. Orthop Res.* 2017. [7] Carlson JA et al. ORS 2018. [8] Carlson JA et al. ORS 2019. [9] Freedman BR et al. *Orthop. Res.* 2015. [10] Beason DP et al. *J. Biomech*, 2012. [11] Dunkman AA et al. *Matrix Biol.* 2013. [12] Favata M, PhD Thesis: University of Pennsylvania. 2006.

ACKNOWLEDGEMENTS: *This study was supported by NIH/NIAMS AR065995 and the Penn Center for Musculoskeletal Disorders (AR069619).*

Limited Scar Resection for Chronic Achilles Repair: Use of a Rat Model

Matthew Counihan MD, Courtney Nuss AS, Joseph Newton BS, Louis Soslowsky PhD, Daniel Farber MD
McKay Orthopaedic Research Laboratory, University of Pennsylvania, Philadelphia, PA
Disclosures: Matthew Counihan MD (N), Courtney Nuss AS (N), Joseph Newton BS (N), Louis Soslowsky PhD (N), Daniel Farber MD (N)

INTRODUCTION: Acute rupture of the Achilles tendon is misdiagnosed in up to 24% of patients [1]. Without acute intervention, the tendon ends retract, the injury gap fills with scar tissue, and treatment becomes more difficult [2]. Current treatment of chronic Achilles tendon ruptures involves debridement of scar tissue back to normal tendon ends, followed by interposition of healthy graft tissue to fill the gap, such as in the gastrocnemius fascia turndown (GFT) technique [3]. Direct repair with the limited scar resection (LSR) technique offers a less invasive alternative, allowing for primary repair of the tendon without a graft, avoiding donor site morbidity [4]. However, LSR has not been adopted as a common surgical alternative due to concern that scar tissue does not heal as well as healthy donor graft tissue. Therefore, the objective of this study was to define and compare the healing properties of the Achilles tendon after chronic injury reconstruction with GFT or LSR, utilizing an animal model to control the injury and treatment strategies. We hypothesized that LSR would have superior healing properties to the GFT and non-repair control groups in a chronic Achilles injury model.
METHODS: *Study Design:* After facility acclimation, 90 male Sprague Dawley rats (400-450g) were used (IACUC approved). Animals were randomized equally into three groups: non-repair (NR), gastrocnemius fascia turndown (GFT), and limited scar resection (LSR). Chronic Achilles injury was generated via unilateral blunt transection of the right Achilles tendon in each rat, followed by 1 week of immobilization of the injured limb in a maximally dorsiflexed position and 5 weeks of cage-activity without immobilization. 6 weeks after the index surgery, GFT and LSR groups underwent chronic Achilles reconstruction. In the GFT technique, all interposed scar tissue was debrided, then the gastrocnemius fascia was flipped on a distal hinge to bridge the gap, reconstructing the tendon. In the LSR technique, a small midsection of the scar tissue was removed to restore the tendon to pre-injury length, followed by end-to-end primary repair of the remaining scar tissue ends. A modified Kessler repair was used in both techniques. The hind limb was immobilized in plantarflexion after the index surgery. Animals were sacrificed at 3 and 6 weeks after repair. The NR group was sacrificed at 9 and 12 weeks from the index procedure to match sacrifice points for all three groups. All rats underwent biweekly in vivo assessments including ambulatory kinetics and kinematics, passive ankle joint mechanics, and ultrasound. Ex vivo assessments included mechanical testing and histology. Cycles to failure comparisons were made using a nonparametric Kruskal-Wallis ANOVA. Other ex-vivo comparisons were made using 1-way ANOVAs. In-vivo assessment comparisons were made using a 2-way ANOVA with repeated measures on time with follow-up t-tests between groups at each time point. Significance was set at $p<0.05$ for all tests.
RESULTS: *Ultrasound*: Ultrasound assessment showed successful post-injury elongation of the Achilles tendon in all groups which is critical to the chronic Achilles injury model. The cross-sectional area of each of the repaired tendons was significantly increased compared to the NR tendons at both time points. The LSR repair had increased vascularity compared to NR in the post-repair period, with increased contrast wash-in rate and decreased contrast time to peak at the 9 week time point. *Mechanical Testing*: Stiffness of LSR and GFT repairs was significantly lower compared to NR at 3 weeks. At 6 weeks, LSR and GFT tendon stiffness improved, such that there was no longer a difference between the three groups. Modulus was significantly lower in both LSR and GFT groups at both 3 and 6 weeks. Cycles to failure (CTF) was significantly higher in NR at 3 weeks as compared to both LSR and GFT. CTF improved in both repair groups at 6 weeks such that there was no longer a difference between the three groups. *Passive Joint Mechanics*: Passive joint mechanics revealed significantly increased dorsiflexion stiffness in the GFT repair group at the first post-repair time point at 8 weeks when compared to NR. LSR repair had increased dorsiflexion stiffness that trended toward significance at the 8 week time point compared to NR. Both LSR and GFT groups had significantly decreased range of motion at the 8 week post-repair time point as compared to NR. *Ambulatory Assessment*: Gait analysis of the GFT and LSR repair groups had significantly decreased ground reaction forces (peak vertical force, peak propulsion forces) as compared to the NR group at the first post-repair assessment 8 week time point. Ground reaction forces were recovered quickly in the LSR group, with no significant difference from the NR group at 10 and 12 weeks. Ground reactive forces for the GFT group remained significantly decreased from the NR group at both 10 and 12 weeks without recovery.
DISCUSSION: The present study supports that both LSR and GFT reconstruction techniques are viable options for treatment of the chronic Achilles tendon injury in a rat model. We established that the injury surgery successfully recreated the elongated Achilles tendon typical of the chronic Achilles injury. Both reconstruction techniques established increased dorsiflexion stiffness and decreased range of motion across the ankle joint. This is representative of the re-establishment of normal length and tension of the Achilles complex in both of the repair groups, which is critical to the success of operative management of a chronic Achilles injury. Ground reaction forces were expectedly decreased after surgery, but quickly recovered in the LSR group, while the GFT group remained significantly decreased through the study. This is reflective of the decreased morbidity incurred by the LSR technique, allowing for a significantly shorter recovery time. Vascular analysis provided evidence of adequate microcirculation and vascularization of this tissue, contesting the notion that a lack of circulation in scar tissue would be a barrier to healing in this technique. Mechanical testing results raise the question of whether these tendons fared better with non-operative management compared to either reconstruction technique. However, it must be noted that at the 3 week and 6 week post-repair sacrifice points, the NR tendons are actually matured to 9 and 12 weeks, respectively. The difference in the relative maturity of the tendon in NR vs GFT/LSR groups inherently introduces a difference in stiffness and strength between the groups. Importantly, the repair groups were able to match the stiffness and strength of the NR group at the 6 week time point, when they have had relatively half the time for healing and scar maturation as the NR group. A limitation of the rat model is that the gastrocnemius muscle of the rat is relatively thinner with a larger soleus as compared to humans, and as such the GFT procedure may cause relatively larger morbidity to the gastrocnemius muscle in the rat.
SIGNIFICANCE: This study supports that the limited scar resection technique is a viable surgical alternative, particularly when minimizing postoperative morbidity and surgical time are paramount. The study also suggests the non-operative management of chronic Achilles injuries may yield similar results as compared to operative management, which necessitates further research into conservative treatment modalities for this condition.
ACKNOWLEDGEMENTS: Funding was provided by the Orthopaedic Research and Education Foundation and the NIH/NIAMS supported Penn Center for Musculoskeletal Disorders (P30AR069619). The authors thank Snehal Shetye, Thomas Leahy, and Harina Raja for their assistance.
REFERENCES: [1] Raikin et al., 2013. Foot Ankle Int. 34:475-80. [2] Bevilacqua et al., 2012. Clin Podiatr Med Surg. 29:291-9. [3] Maffulli et al., 2007. Foot Ankle Clin. 12:583-96. [4] Yasuda et al., 2016. J Bone Joint Surg Am. 98:1168-75.

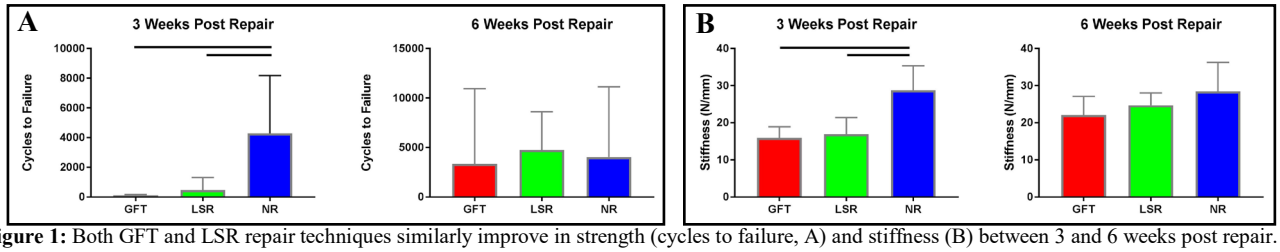

Figure 1: Both GFT and LSR repair techniques similarly improve in strength (cycles to failure, A) and stiffness (B) between 3 and 6 weeks post repair.

Determining the Roles of Decorin and Biglycan in Tendon Healing Using Conditional Deletion at Time of Injury

Ashley K. Fung[1], Stephanie N. Weiss[1], David E. Birk[2], Louis J. Soslowsky[1]
[1]McKay Orthopaedic Research Laboratory, University of Pennsylvania, Philadelphia, PA
[2]Department of Molecular Pharmacology and Physiology, University of South Florida, Tampa, FL
afung@seas.upenn.edu

Disclosures: Ashley K. Fung (N), Stephanie N. Weiss (N), David E. Birk (N), Louis J. Soslowsky (N)

INTRODUCTION: Tendon injury leads to a healing cascade of inflammatory, proliferative, and remodeling phases, but the mechanisms underlying these processes remain unclear. Small leucine-rich proteoglycans (SLRPs) such as decorin (Dcn) and biglycan (Bgn) are regulators of fibrillogenesis and matrix assembly and play important roles throughout tendon healing. Previous studies using conventional *Bgn*$^{-/-}$ and *Dcn*$^{-/-}$ mice showed that absence of Dcn impaired the healing response with no improvement in dynamic modulus between 3- and 6-weeks post-injury, while absence of Bgn had a moderate effect on early tendon healing, together suggesting differential roles of these SLRPs throughout the injury response [1]. However, these results are confounded by the cumulative effects of SLRP deficiency on altered development and growth, and the isolated roles of Dcn and Bgn on tendon healing are unknown. Therefore, the objective of this study was to determine the regulatory role(s) of Dcn and Bgn on the mechanical properties of healing tendons in mature mice using conditional deletion at the time of tendon injury resulting in an isolation of Dcn, Bgn, and both Dcn/Bgn knockdown. We hypothesized that induced deletion of Dcn, Bgn, and both Dcn and Bgn expression would impair the healing response compared to wild type mice leading to reduced improvement in tendon mechanical properties post-injury. Because Dcn has been shown to mediate all stages of healing while Bgn is primarily important in the inflammatory phase, we hypothesized that deletion of Dcn would result in greater impairment.

METHODS: Female *Dcn*$^{+/+}$/*Bgn*$^{+/+}$ control (WT, n=48), *Dcn*$^{flox/flox}$ (I-*Dcn*$^{-/-}$, n=32), *Bgn*$^{flox/flox}$ (I-*Bgn*$^{-/-}$, n=32), and compound *Dcn*$^{flox/flox}$/*Bgn*$^{flox/flox}$ (I-*Dcn*$^{-/-}$/*Bgn*$^{-/-}$, n=32) mice with a tamoxifen inducible Cre (B6.129-Gt(ROSA)26Sortm1(cre/ERT2)Tyj/J, Jackson Labs) were utilized [2] (IACUC approved). At 120 days old, Cre excision of conditional alleles was induced in all mice via two (injured mice) or three (uninjured mice) consecutive daily IP injections of tamoxifen. WT mice also received tamoxifen to account for any potential side effects. WT mice (n=16) were designated as uninjured controls, and remaining mice were divided into 3- or 6-week post-injury groups to represent the early and later remodeling phases of healing (n=16/genotype/time point). At time of induction, mice in injury groups underwent bilateral patellar tendon injury surgery as described [3] and were sacrificed 3- or 6-weeks later. Uninjured groups were sacrificed at 150 days old. The patellar tendon-bone complex from one limb of each animal was dissected and prepared for mechanical testing to assess potential differential effects in both the midsubstance and insertion regions of the tendon [4]. Tendons were subjected to a testing protocol consisting of preconditioning and a quasi-static ramp to failure. Dynamic collagen fiber realignment was measured throughout the ramp-to-failure using a crossed polarizer setup. Images were used to optically measure moduli in the insertion site and midsubstance regions. To evaluate the effect of genotype on tendon healing, one-way ANOVAs with Bonferroni corrections were conducted for 3- and 6-week post-injury groups. Significance was set at $p \leq 0.05$; trends at $p \leq 0.1$.

RESULTS: WT, I-*Dcn*$^{-/-}$, and I-*Bgn*$^{-/-}$ mice had significantly reduced insertion site modulus compared to uninjured controls at both 3- and 6-weeks post-injury, while insertion site modulus was reduced in I-*Dcn*$^{-/-}$/*Bgn*$^{-/-}$ mice only at 6-weeks (Fig. 1A,B). Midsubstance modulus in I-*Dcn*$^{-/-}$ mice was significantly lower than uninjured and I-*Dcn*$^{-/-}$/*Bgn*$^{-/-}$ groups and trended lower compared to I-*Bgn*$^{-/-}$ mice 3-weeks post-injury (Fig 1C). Similarly, midsubstance modulus was significantly lower in I-*Dcn*$^{-/-}$ mice compared to uninjured and I-*Bgn*$^{-/-}$ groups 6-weeks post-injury (Fig 1D). Midsubstance modulus in I-*Dcn*$^{-/-}$/*Bgn*$^{-/-}$ mice also trended lower compared to I-*Bgn*$^{-/-}$ mice (Fig 1D). For failure properties, maximum stress trended lower in I-*Dcn*$^{-/-}$ and I-*Dcn*$^{-/-}$/*Bgn*$^{-/-}$ groups compared to uninjured mice 3-weeks post-injury (Fig 1E), while maximum stress trended lower in I-*Dcn*$^{-/-}$/*Bgn*$^{-/-}$ mice compared to I-*Bgn*$^{-/-}$ mice at 6-weeks (Fig 1F). Finally, normalized circular variance in the midsubstance at 3-weeks was higher (indicating less collagen fiber alignment) in I-*Bgn*$^{-/-}$ and I-*Dcn*$^{-/-}$/*Bgn*$^{-/-}$ groups at strains between 1 and 4%. (Fig 2C). Few differences were observed at the insertion site or at 6-weeks (Fig 2A,B,D).

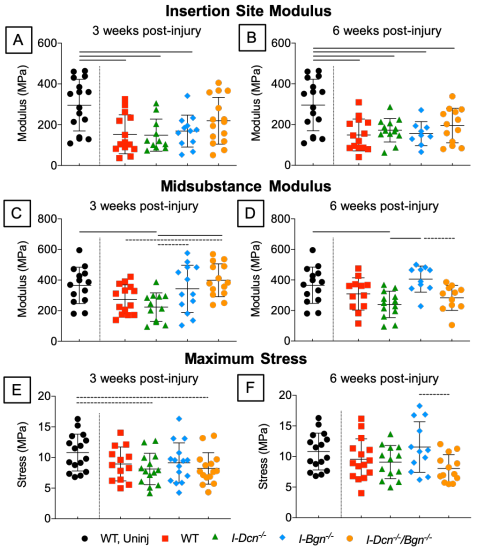

Figure 1: Quasi-static mechanical properties. Insertion site modulus was lower in injured tendons at (A) 3- and (B) 6-weeks post-injury. Only I-*Dcn*$^{-/-}$ groups exhibited reduced midsubstance modulus compared to uninjured at both (C) 3- and (D) 6-weeks post-injury. Maximum stress trended lower in I-*Dcn*$^{-/-}$ and I-*Dcn*$^{-/-}$/*Bgn*$^{-/-}$ compared to uninjured 3-weeks post-injury but (F) not at 6-weeks post-injury. Solid lines denote significance for $p<0.05$ while dashed lines denote trends for $p<0.1$.

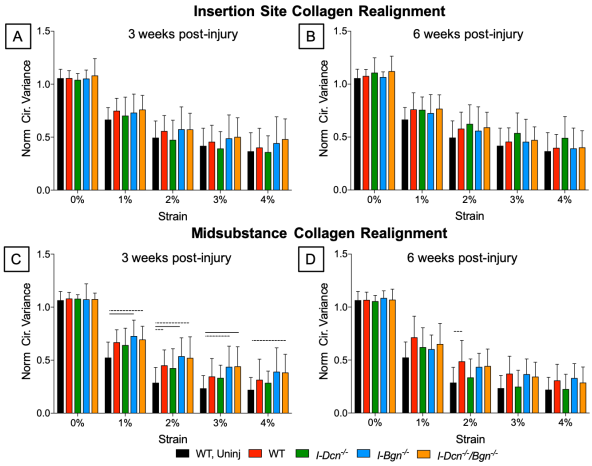

Figure 2: Collagen fiber realignment. There were no differences in collagen fiber realignment at (A) 3- or (B) 6-weeks post-injury within the insertion site region. However, (C) normalized circular variance was higher in I-Bgn$^{-/-}$ and I-Dcn$^{-/-}$/Bgn$^{-/-}$ groups at values of strain between 1 and 4%, and these differences were not sustained to (D) 6-weeks post-injury. Solid lines denote significance for $p<0.05$ while dashed lines denote trends for $p<0.1$.

DISCUSSION: This study investigated the roles for Dcn and Bgn in determining tendon mechanics after injury using conditional deletion of Dcn, Bgn, and both Dcn and Bgn at the time of injury. As hypothesized, results revealed that absence of Dcn negatively impacts tendon healing. Modulus within the midsubstance region, the location where the injury is introduced, was only significantly lower in I-*Dcn*$^{-/-}$ mice at both 3- and 6- weeks post-injury compared to uninjured controls. This healing response is consistent with our previous studies using conventional *Dcn*$^{-/-}$ mice [1], further highlighting the critical role of Dcn in all stages of tendon healing. However, contrary to our hypothesis, induced knockout of Bgn did not impair the healing response compared to WT control animals. These findings contrast those observed in the conventional *Bgn*$^{-/-}$ model suggesting that altered growth, especially considering the important role of Bgn in tendon development and fibrillogenesis, may impair the tendon healing response. Interestingly, midsubstance modulus in I-*Dcn*$^{-/-}$/*Bgn*$^{-/-}$ mice was significantly greater than I-*Dcn*$^{-/-}$ mice 3-weeks post-injury, indicating there may be a compensatory or protective effect for Bgn against detrimental changes due to deletion of Dcn. However, these differences were not evident in the insertion site, suggesting the regulatory roles of decorin and biglycan are regionally dependent. Additionally, increased circular variance in both I-*Bgn*$^{-/-}$ and I-*Dcn*$^{-/-}$/*Bgn*$^{-/-}$ groups in the midsubstance at 3-weeks reveal that deletion of Bgn may alter how fibers in healing tendons respond to changes in load. However, the mechanisms driving differences in tendon modulus during healing remain unknown, and ongoing work to assess changes in gene expression, matrix composition, and fibril structure will further elucidate how Dcn and Bgn impact tendon healing.

SIGNIFICANCE: In contrast to biglycan, induced deletion of decorin at time of injury has a detrimental effect on mechanics of healing tendons. Elucidating the isolated roles of decorin and biglycan in the response to tendon injury will contribute largely to understanding mechanisms that drive poor tendon healing.

REFERENCES: [1] Dunkman AA et al., Ann Biomed Eng, 2014. [2] Robinson et al., Matrix Biology, 2017. [3] Lin et al., J Biomech, 2006. [4] Dunkman AA et al., Matrix Biology, 2013.

ACKNOWLEDGEMENTS: This study was funded by NIH/NIAMS R01AR068057, T32AR007132, and the Penn Center for Musculoskeletal Disorders (P30AR0696919).

Long-Term Nicotine Exposure Alters Rat Supraspinatus Tendon and Bone Properties

Huegel J, Nuss CA, Chan PYW, Cheema AN, Kuntz AF, Soslowsky LJ
McKay Orthopaedic Research Laboratory, University of Pennsylvania, Philadelphia, PA

DISCLOSURES: Huegel J (N), Nuss CA (N), Chan PYW (N), Cheema AN (N), Kuntz AF (N), Soslowsky LJ (N)

INTRODUCTION: Nicotine is a well-established risk factor for rotator cuff injuries [1]. Several laboratory studies showed that nicotine negatively impacts tendon healing after injury, in both the rat rotator cuff [2] and Achilles [3]. Surprisingly, after twelve weeks of nicotine exposure, material properties of the uninjured rat supraspinatus tendon had increased maximum stress and elastic modulus compared to controls [4]. Conversely, nicotine decreased bone mass due to imbalanced bone turnover [5]. However, an understanding of nicotine effects on rotator cuff tendon-to-bone properties after long term exposure is lacking. Therefore, the objective of this study is to investigate the effects of eighteen weeks of nicotine exposure on tendon-to-bone properties in a rat model via mechanical, μCT, and histological analyses. We hypothesized that long term nicotine exposure would lead to decreased tendon mechanical properties, decreased subchondral bone insertion properties, and decreased trabecular bone properties in the humeral head, as well as altered tendon cell morphology.

METHODS: 24 adult male Sprague-Dawley rats (350-400g) were used (IACUC approved). Animals were randomized to receive either 0.9% sterile saline (n=12) or 61 mg/ml nicotine (n=12) through subcutaneously implanted osmotic pumps, which correlated with appropriate levels of cotinine measured in the blood serum (400-700 ng/ml) [3]. Rats were sacrificed after 18 weeks of exposure. Animals were stored at -20°C until supraspinatus tendon-humerus complexes were dissected out and processed for histological analysis (n=5, right limbs) or cross-sectional area measurement and quasistatic mechanical testing (n=12, left limbs). Testing consisted of pre-conditioning, stress relaxation at 5% strain, and a quasi-static ramp to failure at 0.3%/s. Post-test, humeri were μCT scanned at 6μm resolution to assess trabecular properties of the epiphysis proximal to the humeral growth plate, representing the region of rotator cuff attachment on the greater tuberosity. Additionally, the mineralization gradient was calculated (Amira 6.7) across the subchondral plate, defined as the mineralized fibrocartilage of the supraspinatus tendon enthesis and subchondral bone. Briefly, a 100x120x230 voxel volume was identified in the greater tuberosity at the supraspinatus tendon insertion site. After thresholding, the innermost layer of the subchondral bone was defined. Individual layers were then defined outwards towards the mineralized fibrocartilage boundary. Layer intensity values were averaged to construct a mineralization gradient, normalized to the total subchondral plate thickness. Intensity was compared at normalized thickness of 0, 0.5, and 1.0, marking the boundaries between trabecular bone, subchondral bone, mineralized fibrocartilage, and tendon. Statistical comparisons were made between the saline and nicotine groups. Comparisons for mechanics and μCT metrics were made using Student's t-tests. Mineralization intensity was also compared with two-way ANOVA across subchondral thickness. Histological comparisons were made using Mann-Whitney tests. Significance was set at $p<0.05$ (solid bars), and trends at $p<0.1$ (dashed bars).

RESULTS: *Mechanical properties*: Tendons in the nicotine group had a smaller cross-sectional area than the saline group (Fig 1A). There were no differences in stress relaxation (not shown) or tissue modulus measured through the length of the tendon (Fig 1B). However, the nicotine group showed a trend toward decreased modulus at the insertion (first 2 mm proximal to the insertion, Fig 1C), as well as significantly decreased tendon stiffness (Fig 1D). *Histological measures*: No differences were seen at the tendon insertion in cellularity or cell shape (Fig 2A,B). However, cell density in the midsubstance was decreased with nicotine exposure (Fig 2C); cell shape was not different (Fig 2D). Representative images of each region are shown in Figure 2E. *μCT parameters*: Although no differences were identified in bone volume fraction or trabecular thickness (Fig 3A,B), there was a trend toward increased trabecular number and decreased separation (Fig 3C, D). Additionally, mineralization intensity was significantly different across the subchondral plate between treatment groups, although not when specific comparisons were made at locations of interest (0, 0.5, and 1.0 thicknesses; Fig 3E).

DISCUSSION: This study measured the effects of long-term nicotine exposure on uninjured supraspinatus tendon and underlying humeral bone properties. Previous work found that nicotine caused decreased Achilles tendon cross-sectional area after injury [3]; similarly, nicotine-exposed animals had smaller uninjured supraspinatus tendons, suggesting a potential decrease in metabolic activity, consistent with decreased cell density in the current study. Contrary to previous reports [4], this study demonstrated decreased tendon mechanical properties, supporting clinical findings and highlighting the importance of time course studies. Surprisingly, trabecular bone properties were slightly improved with nicotine exposure, suggesting that bone metabolism is also affected, though potentially not as hypothesized. Future studies will investigate additional time points as well as kinetic bone histomorphometry. Although data was variable, increased bone mineralization intensity at the tendon insertion could increase stress concentrations across the tendon-bone interface, increasing risk of tendon rupture [6]. Physical activity such as exercise or overuse may produce more dramatic changes to the tendon structure and composition.

SIGNIFICANCE: This study demonstrates that nicotine leads to decreased mechanical properties in uninjured supraspinatus tendons as well as alterations in bone structure. Patients should be counseled that use of nicotine increases their risk of tendon degeneration and may predispose them to tendon injury.

REFERENCES: [1] T. Hu et al. *Tob. Control*, 9:II60-3. 2000. [2] Galatz LM et al. *J Bone Joint Surg (Am)*, 88:2027-34. 2006. [3] Cheema AN et al. *J Orthop Res*, 37: 94-103. 2019. [4] Ininose R et al. *Acta Orthopaedica*, 81:634-638. 2010. [5] Cusano E. Curr Osteoporos Rep, 13:302-309. 2015. [6] Genin GM et al. Biophys K, 2009.

ACKNOWLEDGEMENTS: Funding was provided by the NIH/NIAMS supported Penn Center for Musculoskeletal Disorders (P30 AR069619). We thank Ashley Fung for help with μCT assays.

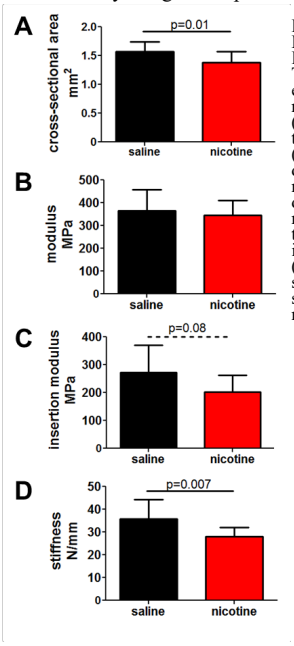

Figure 1. Mechanical Properties. Tendons exposed to nicotine had (A) decreased tendon area, (B) no difference in modulus, (C) decreased modulus at the tendon insertion, and (D) decreased stiffness. Data shown as mean+SD.

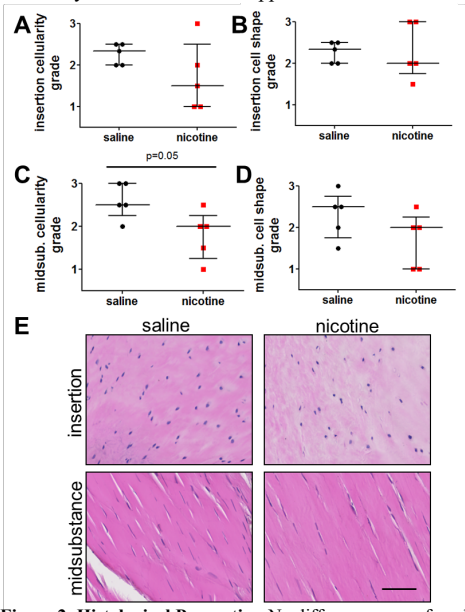

Figure 2. Histological Properties. No differences were found between groups for (A) insertion cellularity or (B) insertion cell shape. Nicotine tendons had (C) decreased cellularity in the midsubstance, but (D) cell shape was not changed. (E) Representative regions of interest at 200x magnification. Data shown as median±IQR. Scale bar: 100 μm.

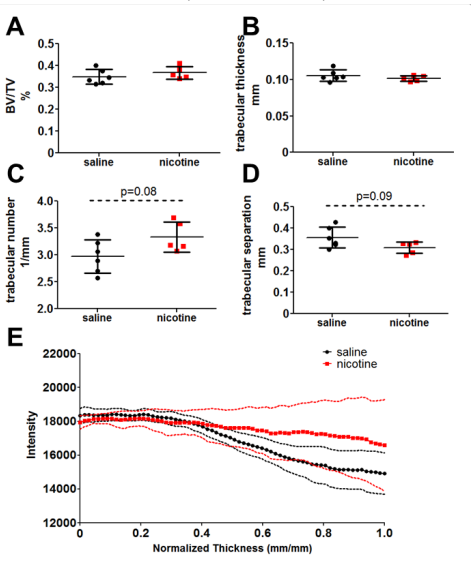

Figure 3. μCT Properties. Nicotine did not have an effect on (A) trabecular bone fraction or (B) trabecular thickness in the humeral epiphysis. (C) Trabecular number was increased and (D) trabecular separation was decreased in nicotine treated rats. (E) Bone mineralization (intensity) across the subchondral plate from the trabecular boundary (0) to the tendon boundary (1.0) was different between groups ($p<0.04$). Data shown as mean±SD.

Mechanisms of Action of Pulsed Electromagnetic Field Therapy on a Rat Model of Rotator Cuff Injury and Repair

Huegel J[1], Weiss SN[1], Nuss CA[1], Raja H[1], Waldorff EI[2], Zhang N[2], Ryaby JT[2], Soslowsky LJ[1], Kuntz AF[1]
[1]McKay Orthopaedic Research Laboratory, University of Pennsylvania, Philadelphia, PA [2]Orthofix Inc., Lewisville, TX

DISCLOSURES: Huegel J (N), Weiss SN (N), Nuss CA (N), Raja H (N), Waldorff EI (3A,4-Orthofix, Inc.), Zhang N (3A,4-Orthofix, Inc.), Ryaby JT (3A,4-Orthofix, Inc.), Soslowsky LJ (5-Orthofix, Inc.), Kuntz AF (5-Orthofix, Inc.)

INTRODUCTION: Rotator cuff tears affect millions of individuals each year, often requiring surgical intervention. Although advancements in surgical and rehabilitation protocols have improved clinical results, rotator cuff repair failure is common [1]. To improve surgical outcomes, non-invasive therapies have been utilized post-operatively [2]. We have previously shown that pulsed electromagnetic field (PEMF) therapy improved tendon-to-bone mechanical properties in a rat model of rotator cuff injury and repair [3,4], consistent with increased type I collagen and fibronectin protein expression and increased collagen alignment [4], potentially providing an explanation for the improved mechanical properties. However, these alterations in composition and tissue structure could be downstream of specific physiological responses to PEMF treatment, including changes in inflammation, cell signaling, cell metabolism, increased production of matrix components, and/or changes in matrix degradation and remodeling [5]. Therefore, the objective of this study was to determine the influence of PEMF treatment on tendon gene expression and cell composition during early stages of healing. We hypothesized that PEMF treatment would amplify tendon-healing related signaling pathways such as TGF-β while mitigating inflammation.

METHODS: 106 adult male Sprague-Dawley rats (400-450g) were used (IACUC approved). Animals underwent acute supraspinatus injury and repair [3] followed by systemic exposure to Physio-Stim® PEMF (Orthofix, Inc.) for 1 hour daily. Control animals did not receive PEMF therapy (non-PEMF). Animals were euthanized at 3, 7, 14, 21, or 28 days post-op (n=10/group/time point). From half of the animals, right supraspinatus tendons were dissected out and divided into insertion and midsubstance portions for RNA isolation, cDNA synthesis, specific target amplification, and Fluidigm qPCR for 40 target genes and 2 housekeeping genes (n=5/group/time point). Expression was normalized to the housekeeping genes and then to non-PEMF at each time point. From the other half of the animals, right shoulders were dissected and processed for histological analysis. H&E stained sections were semi-quantitatively graded for cell density (cellularity) and cell shape [3,4](n=5/group/time point), and CD68 and CD163 immunohistochemical staining was performed for M1 and M2 macrophages, respectively (n=4/group at 14 and 28 days). Statistical comparisons were made between PEMF and non-PEMF groups over time and at each time point, using two-way ANOVAs with Bonferroni post-hoc tests. Immunohistochemical staining was qualitatively assessed in a blinded manner.

RESULTS: *Gene expression:* Expression of the BMP2 signaling molecule was increased with PEMF treatment in the tendon insertion across time (Fig 1A); downstream targets collagen type 1a (Fig 1B), alkaline phosphatase (Fig 1C), and osteocalcin (Fig 1D) were also upregulated with PEMF. Although transforming growth factor (TGF) β1 and 2 were unchanged (data not shown), expression of TGFβ3 was downregulated with PEMF treatment in the tendon insertion (Fig 1E). Matrix metalloproteinase (MMP) 9 and connective tissue growth factor (CTGF) were upregulated early and downregulated late (Fig 1F,G), and MMP13 was downregulated across time (not shown). Fibronectin expression increased in PEMF treated tendons (Fig 1H). Similar expression patterns of TGFβ3, MMP9, and fibronectin were seen in the tendon midsubstance (not shown). Expression of inflammatory markers was also altered with PEMF, including increased interleukin-10 and tachykinin (Fig 2A,B), and decreased interleukin-1β and tumor necrosis factor α (Fig 2C,D). *Immunohistochemistry:* At 14 days, CD68+ (M1) macrophages were increased in the midsubstance of non-PEMF tendons (Fig. 2E, top panel). No differences were seen at 28 days, or in the insertion (not shown). CD163+ (M2) macrophages were increased in the insertion of PEMF tendons at 14 days (Fig 2E, bottom) with no differences seen at 28 days or in the midsubstance (not shown). *Histology*: There were no differences in cell density or cell shape in either the tendon insertion or midsubstance with PEMF treatment compared to non-PEMF controls (Fig 3). Cell shape and cellularity varied over time in the midsubstance for both groups, but did not significantly change in the insertion.

DISCUSSION: This study demonstrated molecular and cellular changes within supraspinatus tendons after injury with PEMF treatment. Gene expression data suggests an upregulation in the BMP2 signaling pathway, including increased collagen production during early healing. Increases in pro-osteogenic genes at the insertion could support important processes to re-establish the tendon-bone interface. Future work will assess kinetic bone properties in the greater tuberosity. Decreased TGFβ3 and changes in MMP expression support a downregulation in the fibrotic response with PEMF, which coincides with a decreased tendon cross-sectional area at 4 weeks seen in previous studies [4]. Interestingly, PEMF had a consistent anti-inflammatory effect, upregulating *Il10* and *Tac1*, and downregulating *Il1β* and *Tnfα*, as well as a decrease in CD68+ macrophages and increase in CD163+ macrophages at 14 days in PEMF-treated tendons. Similar mechanisms have been shown in intervertebral disc cells after PEMF treatment *in vitro* [5] and *in vivo* [6]. Although statistical comparisons were not made, regional differences in gene expression and cell morphology support the need to assess tendon responses regionally.

SIGNIFICANCE: Previous work showing improved rotator cuff healing with PEMF supported the initiation of a PEMF clinical trial for this condition. This study provides important mechanistic insight into how PEMF affects cellular and molecular processes in the supraspinatus tendon after injury.

REFERENCES: [1] Galatz LM et al. J Bone Joint Surg Am, 2004. [2] Lovric V et al. Knee Surg Sports Traumatol Arthrosc, 2013. [3] Tucker JJ et al. J Orthop Res, 2016. [4] Huegel J et al. J Shoulder Elbow Surg, 2018. [5] Miller SL et al. Spine J, 2016. [6] Tang X et al. ORS 2017.

ACKNOWLEDGEMENTS: Funding was provided by Orthofix, Inc. and the Penn Center for Musculoskeletal Disorders (P30 AR069619). We thank Dr. Matthew Counihan, Dr. Yaping Ye, Peter Chan, and the Penn Molecular Profiling Facility for their assistance.

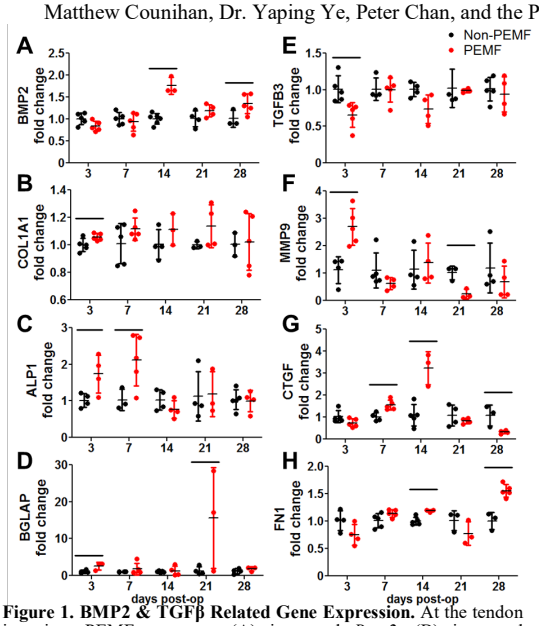

Figure 1. BMP2 & TGFβ Related Gene Expression. At the tendon insertion, PEMF treatment (A) increased *Bmp2*, (B) increased *Col1a1*, (C) increased *Alp1*, (D) increased *Bglap*, (E) decreased *Tgfβ3*, (F) altered *Mmp9*, (G) increased *Ctgf*, and increased (F)*Fn1*. Data shown as mean±SD, normalized to housekeeping and then normalized to non-PEMF at each time point (n=5/group/time point).

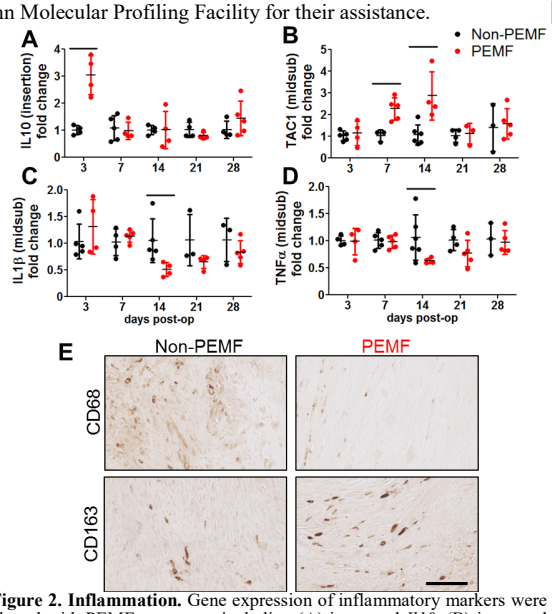

Figure 2. Inflammation. Gene expression of inflammatory markers were altered with PEMF treatment, including (A) increased *Il10*, (B) increased *Tac1*, (C) decreased *Il1β*, and (D) decreased *Tnfα*. Representative 200x images show (E, top) decreased CD68+ staining at the midsubstance and (E, bottom) increased CD163+ staining at the insertion at 14 days post-op in PEMF tendons. Scale bar: 100 μm.

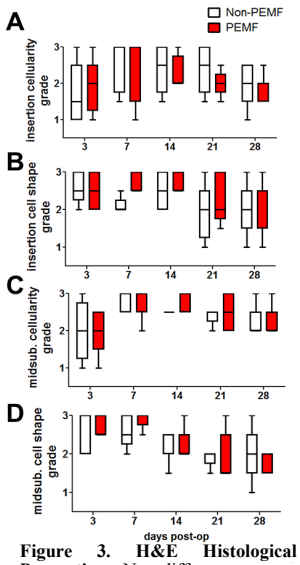

Figure 3. H&E Histological Properties. No differences were found between groups for (A) insertion cellularity, (B) midsubstance cellularity, (C) insertion cell shape, or (D) midsubstance cell shape. Midsubstance properties were altered over time. Data shown as median+IQR.

The Differential Roles of Decorin and Biglycan in the Early Proliferative and Remodeling Phases of Tendon Healing

Thomas P. Leahy[1], Ashley K. Fung[1], Stephanie N. Weiss[1], David E. Birk[2], Louis J. Soslowsky[1]
[1]McKay Orthopaedic Research Laboratory, University of Pennsylvania, PA
[2]Department of Molecular Pharmacology and Physiology, University of South Florida, Tampa, FL
tpleahy@seas.upenn.edu.

Disclosures: Thomas P. Leahy (N), Ashley K. Fung (N), Stephanie N. Weiss (N), David E. Birk (N), Louis J. Soslowsky (N)

INTRODUCTION: Tendon matrix consists of highly organized collagen fibrils with small leucine rich proteoglycans (SLRPs) bound to the fibril surface. SLRPs decorin and biglycan play a critical role in regulating tendon healing processes. Specifically, using conventional *Bgn*$^{-/-}$ and *Dcn*$^{-/-}$ mice, the absence of biglycan diminished initial tendon healing following injury while the absence of decorin reduced late tendon healing.[1] However, these studies have confounding effects due to the absence of decorin and biglycan during development[2] and do not allow the roles of these SLRPs to be defined at specific phases (inflammation, proliferation, remodeling) of healing. Therefore, the objective of this study was to define the roles of decorin and biglycan in specific healing phases using inducible knockouts. We hypothesized that a complete knockout (i.e., a Bgn-Dcn double knockout) earlier in the healing process would have the greatest negative effect since both SLRPs would be absent throughout the proliferative and remodeling phases. Further, we hypothesized that decorin knockout would result in more pronounced negative effects on healing compared to biglycan knockout regardless of time of induction and that decorin knockout would reduce tendon healing similarly when knocked out during early or late stage healing due to its known role in the later remodeling phase.

METHODS: Study Design: Female wildtype (WT, n=48), *Dcn*$^{flox/flox}$ (I-*Dcn*$^{-/-}$, n=48), *Bgn*$^{flox/flox}$ (I-*Bgn*$^{-/-}$, n=48), and compound *Dcn*$^{flow/flox}$/*Bgn*$^{flox/flox}$ (I-*Dcn* $^{-/-}$/*Bgn*$^{-/-}$, n=48) mice with a tamoxifen (TM) inducible Cre, (B6.129-Gt(ROSA)26Sortm1(cre/ERT2)Tyj/J, Jackson Labs) were utilized (IACUC approved). At maturity (120 days), mice underwent bilateral patellar tendon injury surgery as described.[1,3] Following surgery, Cre excision of the conditional alleles was induced via two consecutive daily IP injections of tamoxifen (2 mg/40g body weight). WT mice received tamoxifen injections at 120 days and were evenly divided between the uninjured control group, which were sacrificed at 150 days, and surgery groups which were sacrificed at 3 or 6 weeks post-injury, representing the early remodeling and mid-remodeling phases of tendon healing, respectively. Mice from knockout genotypes underwent surgery and were evenly divided between Cre-induction during the early proliferative period (tamoxifen injections beginning at 5 days, termed TM5) or during the remodeling period (tamoxifen injections beginning at 21 days, termed TM21). TM5 animals were sacrificed at 3 or 6 weeks post-injury, while TM21 mice were sacrificed at 6 weeks post-injury (n=16/genotype/induction timepoint/sacrifice timepoint). Mechanical Testing Protocol: The patellar tendon-bone complex from one limb of each animal was dissected and prepared for mechanical testing. Tendons were then subjected to mechanical testing consisting of preconditioning followed by a quasi-static ramp to failure. Material properties of the tendons were calculated from the load-displacement data via optical tracking of stain lines on the tendon using MATLAB. Throughout mechanical testing, dynamic collagen fiber realignment was quantified using cross-polarization imaging, and regional fiber alignment data was interpolated with a polynomial fit as a function of strain from the load-displacement data between 0 and 4% tendon strain. Statistics: Comparisons were made between genotypes and the relevant uninjured and WT controls at each induction timepoint-sacrifice timepoint combination (TM5-3wk, TM5-6wk, and TM21). Mechanical properties were compared with three separate one-way ANOVAs with Bonferroni post-hoc corrections with significance at $p \leq 0.05$ and trends at $p \leq 0.1$. Fiber realignment properties were compared between strain levels and genotypes with a two-way ANOVA. If the effect of strain level or genotype was significant, a one-way ANOVA with Bonferroni post hoc corrections was performed (if strain had a significant effect, multiple comparisons were made from 0% strain to all strain levels and between adjacent strain levels) with significance set at $p \leq 0.05$.

RESULTS: Injury significantly reduced modulus at both 3 and 6 weeks in the WT tendons (Fig 1). Decreased modulus was maintained in both the TM5 I-*Dcn*$^{-/-}$ and TM5 I-*Dcn*$^{-/-}$/*Bgn*$^{-/-}$ groups but not in the TM5 I-*Bgn*$^{-/-}$ group at either 3 or 6 weeks. In the TM21 groups, a decreased modulus was maintained in the I-*Dcn*$^{-/-}$ group with a trending decrease in the I-*Bgn*$^{-/-}$ group and no difference between the uninjured and I-*Dcn*$^{-/-}$/*Bgn*$^{-/-}$ groups. There were no changes in max stress with injury or between genotypes, except for a trending decrease in max stress at 6 weeks in the I-*Dcn*$^{-/-}$ group (data not shown). All tendons showed significantly increased fiber realignment with increasing strain in both the insertion and midsubstance regions (Fig 2, insertion data not shown). There were no differences in realignment between genotypes, except in the midsubstance region of the TM5 I-*Dcn*$^{-/-}$ tendons at 6 weeks, which showed significantly less realignment relative to the uninjured control.

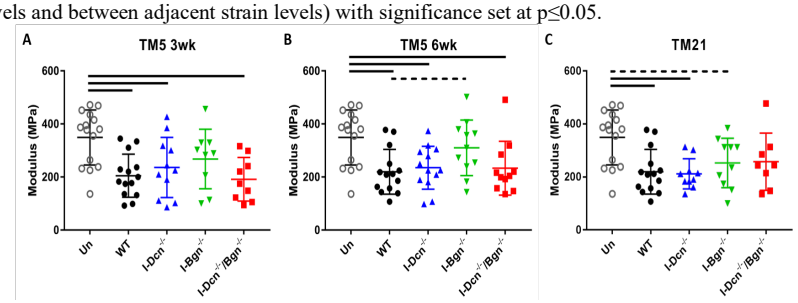

Figure 1. Tendon modulus comparisons at TM5-3wk (A), TM5-6wk (B), and TM21 (C). The TM5 I-*Bgn*$^{-/-}$ group abolished differences with injury, while TM5 and TM21 I-*Dcn*$^{-/-}$ groups showed consistent effects on mechanics. Solid bars represent significance ($p \leq 0.05$) and dotted bars represent trends ($p \leq 0.1$).

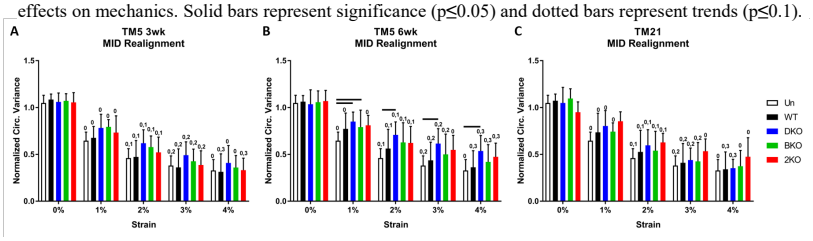

Figure 2. Midsubstance realignment data for TM5-3wk (A), TM5-6wk (B), and TM21 (C). All groups showed increased alignment with increasing strain. TM5 I-*Dcn*$^{-/-}$ group showed altered fiber realignment behavior relative to uninjured. Solid bars represent significance ($p \leq 0.05$) between genotypes. Numbers above indicate significance from noted strain values given the comparisons performed (see methods).

DISCUSSION: Contrary to our hypothesis, the TM5 I-*Dcn*$^{-/-}$/*Bgn*$^{-/-}$ and TM21 I-*Dcn*$^{-/-}$/*Bgn*$^{-/-}$ groups did not exhibit significantly reduced tendon healing at 3 or 6 weeks relative to the WT control. Moreover, decorin knockout did not show a significant negative effect on tendon mechanics compared to biglycan knockout at either TM5 or TM21. Interestingly, biglycan knockout appeared to reduce the negative effects of tendon injury, as there were no negative mechanical effects of injury at 3 or 6 weeks in the TM5 I-*Bgn*$^{-/-}$ tendons. Further, these results suggest that biglycan plays a negative role in early healing, as TM21 I-*Bgn*$^{-/-}$ had negative changes with injury not present in TM5 I-*Bgn*$^{-/-}$. Finally, while TM5 I-*Dcn*$^{-/-}$ and TM21 I-*Dcn*$^{-/-}$ had similar effects on tendon mechanics as hypothesized, TM5 I-*Dcn*$^{-/-}$, but not TM21 I-*Dcn*$^{-/-}$, showed altered fiber realignment behavior at 6 weeks, suggesting that decorin plays a role in regulating fiber organization in early stage tendon healing. These results contrast with previous studies using conventional knockout mice that suggested that *Bgn*$^{-/-}$ mice had impaired early tendon healing and *Dcn*$^{-/-}$ mice had clearly diminished late stage tendon healing,[1] underscoring the importance of using inducible animals to distinguish the specific temporal roles of these SLRPs in tendon healing. Future work will elucidate the underlying mechanisms behind altered tendon healing with temporal deletion of decorin and biglycan by investigating gene expression, matrix composition, and fibril structure in these tendons.

SIGNIFICANCE: This study used novel inducible knockout mice for decorin and biglycan to investigate the temporal roles of these SLRPs during the early proliferative and remodeling phases of tendon healing. This data suggests that biglycan plays a significant negative role in tendon healing, particularly in the early proliferative phase, while decorin does not play a drastic temporal role in tendon healing.

ACKNOWLEDGEMENTS: We acknowledge financial support from NIH/NIAMS (R01AR068057 and P30AR069619).

REFERENCES: 1. Dunkman *et al. Ann. Biomed. Eng.* 42, 201. 2. Dourte *et al. J. Orthop. Res.* 31, 2013. 3. Dunkman *et al. Matrix Biol.* 35, 2014.

Collagen V Deficiency during Healing Mitigates the Quasi-Static Mechanical Deficits of Injured Tendons

Ryan J Leiphart[1], Stephanie N Weiss[1], David E Birk[2], Louis J Soslowsky[1]
[1]McKay Orthopedic Research Laboratory, University of Pennsylvania, Philadelphia, PA
[2]Department of Molecular Pharmacology and Physiology, University of South Florida, Tampa, FL

Disclosures: RJ Leiphart (N), SN Weiss (N), DE Birk (N), LJ Soslowsky (N)

INTRODUCTION: Classic Ehlers-Danlos Syndrome (cEDS) is characterized by genetic mutations of collagen V, a matrix protein present in tendon [1]. Two hallmarks of cEDS are connective tissue hyperelasticity and poor wound healing, and a murine model of cEDS demonstrates impaired tendon healing [2,3]. It is unknown whether this impaired healing response is due to the regulatory role of collagen V during tendon healing or due to pre-existing differences in collagen V-deficient tendons. Therefore, the objective of this study was to determine the isolated role of collagen V on healing tendon mechanics. Due to its role in fibrillogenesis, we hypothesized that acute knockout of collagen V following injury would result in decreased tendon mechanical properties at both intermediate and late healing time points.

METHODS: *Animals*: Male wild-type (WT) (n=45) and bitransgenic *Col5a1*$^{flox/+}$ (n=30) and *Col5a1*$^{flox/flox}$ (n=30) mice with a tamoxifen (TM)-inducible Cre were used in this study (IACUC approved). At 120 days old, mice received bilateral, full thickness, partial width patellar tendon injuries under sterile conditions [4]. For Cre-mediated excision of the *Col5a1* gene, mice received two consecutive daily doses of TM (2mg/40g body weight) beginning on the day of injury. Mice were sacrificed at 3 or 6 weeks post-injury. Healthy WT control mice received TM doses (3 days of 4mg/40g body weight) at 120 days old and were sacrificed 30 days later. Tibia-patellar tendon-patella complexes were harvested and prepared for mechanical testing as previously described [5]. *Mechanical Testing*: Uniaxial, viscoelastic testing was performed with an Instron 5848. The testing protocol consisted of 10 cycles of preconditioning, followed by stress relaxations at 3%, 4%, and 5% strain. Following each stress relaxation, frequency sweeps of 10 cycles at 0.1, 1, 5, and 10Hz were performed. A ramp-to-failure followed the 5% stress relaxation. Percent relaxation, dynamic modulus (E*), and phase shift (δ) were quantified for each stress relaxation and frequency sweep. Stiffness, modulus, maximum load, and maximum stress were quantified from the ramp-to-failure data. *Statistics*: For all mechanical properties, one-way ANOVAs with Bonferroni post-hoc tests were used to compare across genotypes and uninjured controls at each healing time point. Significance was set at $p \leq 0.05$, and trends were set at $p \leq 0.1$.

RESULTS: ***Injury effects:*** Compared to uninjured tendons, injured WT tendons had increased cross-sectional area (CSA) (Fig 1). *Quasi-Static Mechanics*: Compared to uninjured tendons, injured WT tendons were less stiff (Fig 2A), had no differences in max load (data not shown), had decreased modulus (data not shown), and lower max stress (Fig 2B). *Stress Relaxation*: Compared to uninjured tendons, injured WT tendons had greater stress relaxation at 3%, 4%, and 5% strains (data not shown). *Dynamic Mechanics*: Compared to uninjured tendons, injured WT tendons had decreased dynamic moduli at all strains and frequencies, larger tan(δ) values at 3 and 4% strain and for most frequencies at 5% strain for 6-week WT tendons (data not shown). ***Genotype effects:*** Injured *Col5a1*$^{+/-}$ (HET) and *Col5a1*$^{-/-}$ (NULL) tendons had increased CSA relative to uninjured (Fig 1). At 3 weeks post-injury, NULL tendons had decreased CSA relative to WT and a trend towards smaller CSA relative to HET. *Quasi-Static Mechanics*: No differences in stiffness were observed between HET and uninjured tendons (Fig 2A). HET tendons trended towards higher stiffness relative to injured WT tendons at both healing time points. 3-week NULL tendons were less stiff than uninjured tendons, but this decrease did not persist at 6-weeks. 3-week HET tendons had lower max stress than uninjured tendons, but this decrease did not persist at 6-weeks (Fig 2B). 3-week NULL tendons had lower max stress than uninjured tendons, and this difference persisted as a trend at 6-weeks. 3-week NULL tendons had higher max stress than 3-week WT tendons and trended towards higher max stress relative to 3-week HET tendons. HET and NULL tendons had decreased modulus compared to uninjured. No differences in max load were observed between knockout and uninjured tendons. No differences in max load or modulus were observed between injured genotypes. *Stress Relaxation*: HET and NULL tendons had increased stress relaxation at 3% and 4% strain relative to uninjured. 3-week HET and NULL tendons exhibited increased stress relaxation at 5% strain relative to uninjured, which persisted for 6-weeks HET but not for 6-week NULL tendons. No differences in stress relaxation were observed between injured genotypes at any strain. *Dynamic Mechanics*: HET and NULL tendons had decreased dynamic moduli relative to uninjured. For most frequencies at 3% and 4% strain, HET and NULL tendons had larger tan(δ) values than uninjured, while at 5% strain, 6-week HET tendons had larger tan(δ) values than uninjured. No differences in tan(δ) values were observed between 6-week NULL and uninjured tendons. No differences in dynamic modulus or tan(δ) values were observed between injured genotypes at any strain or frequency.

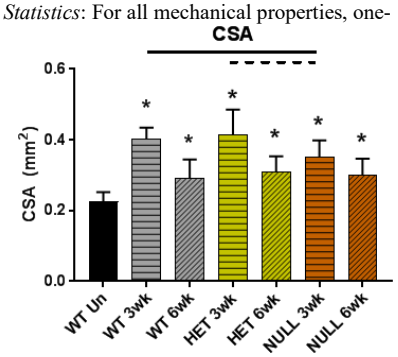

Fig 1. Cross-sectional area. Injured tendons across all genotypes and healing time points had larger CSA than uninjured tendons. * indicates $p \leq 0.05$ compared to uninjured tendons. Solid bars indicate $p \leq 0.05$, and dashed bars indicate $p \leq 0.1$.

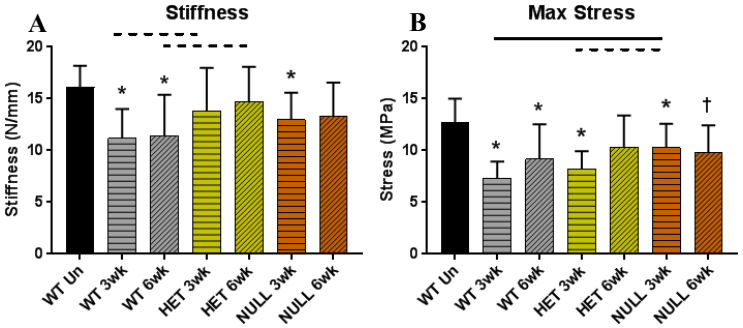

Fig 2. Quasi-static properties. (A) HET tendons had no differences in stiffness compared to uninjured tendons but trended towards higher stiffness compared to WT at both healing time points. (B) 6-week HET tendons had no differences in max stress compared to uninjured tendons. * indicates $p \leq 0.05$, and † indicates $p \leq 0.1$, compared to uninjured tendons. Solid bars indicate $p \leq 0.05$ and dashed bars indicate $p \leq 0.1$.

DISCUSSION: Injured tendons exhibited substantial deficits in mechanical properties relative to uninjured tendons. Contrary to our hypothesis, however, acute knockout of collagen V did not further impair the mechanical properties of these healing tendons. Instead, stiffness did not decrease through healing in HET tendons. Injured HET tendons were stiffer than WT tendons at each healing time point. No decreases in max stress were seen with 6-week HET tendons. These results demonstrate that while healing tendons have impaired mechanical properties, collagen V deficiency during healing does not further diminish these properties. Instead, collagen V haploinsufficiency during healing mitigated the decreases in stiffness and max stress seen in WT injured tendons. Impaired tendon healing in cEDS patients may not be due to the regulatory role of collagen V during healing and may instead be due to pre-existing deficiencies of the tissue. A previous study found that fibroblasts from a murine model of cEDS demonstrated decreased proliferation, migration, and wound healing relative to WT fibroblasts [6]. Results of the present study support the notion that poor wound healing in cEDS patients is due to differences in tissue properties that existed prior to injury. A limitation of this study is the global nature of the collagen V knockouts, which could cause confounding effects on neighboring tissues. The inducible knockout models used here lessen these effects due to the short period of knockout. Future studies will analyze the composition and gene expression of these tendons to identify other differences in healing, collagen V-deficient tendons. Overall, this study demonstrates that collagen V deficiency does not impair the mechanical properties of injured tendons beyond the normal healing response, and instead mitigates some of these mechanical deficits.

SIGNIFICANCE: This study reveals that the quasi-static mechanical deficits of injured tendons are not worsened, and are instead mitigated, by collagen V deficiency. These results provide a further understanding of the role of collagen V in tendon healing.

REFERENCES: [1] Symoens S et al. *Hum Mutat*. 2012. [2] Malfait F & De Paepe A. *AEMB*. 2014. [3] Johnston JM et al. *JOR*. 2017. [4] Beason DP et al. *J Biomech*. 2012. [5] Dunkman AA et al. *Matrix Biol*. 2013. [6] DeNigris J et al. *Connect Tissue Res*. 2016.

ACKNOWLEDGEMENTS: This work was supported by the NIH (R01AR065995, P30AR069619) and the NSF GRFP.

Acute Reduction in Collagen V Expression Increases Viscoelasticity in Mature Tendons

Ryan J Leiphart[1], Stephanie N Weiss[1], David E Birk[2], Louis J Soslowsky[1]
[1]McKay Orthopedic Research Laboratory, University of Pennsylvania, Philadelphia, PA
[2]Department of Molecular Pharmacology and Physiology, University of South Florida, Tampa, FL

Disclosures: RJ Leiphart (N), SN Weiss (N), DE Birk (N), LJ Soslowsky (N)

INTRODUCTION: Classic Ehlers-Danlos Syndrome (cEDS) is a disease caused by mutations in the gene encoding collagen V, a fibrillogenic protein present in tendon [1]. cEDS patients experience joint hypermobility, which is likely caused by connective tissue dysregulation in the absence of collagen V [2]. Tendon-specific knockout of collagen V decreases tendon mechanical properties due to an aberrant development of tissue fibrils [3]. However, the regulatory role of collagen V in tendon homeostasis has not been distinguished from its role in development. Understanding this homeostatic role is critical for establishing the baseline effect of collagen V knockdown in both healthy and injured mature tendons. Therefore, the objective of this study was to determine the effect of acute knockdown of collagen V on the mechanical properties of mature tendons. Since the tendon fibril network is well-established by tissue maturity, we hypothesized that acute knockdown of collagen V in mature tendons would result in minimal changes to tendon mechanical properties.

METHODS: *Animals*: Male wild-type (WT) (n=15) and bitransgenic *Col5a1*$^{flox/+}$ (n=15) and *Col5a1*$^{flox/flox}$ (n=15) mice with a tamoxifen (TM)-inducible Cre were used in this study (IACUC approved). At 120 days old, mice received 3 consecutive daily TM doses (4mg/40g body weight) for Cre-mediated excision of the *Col5a1* gene. Mice were sacrificed 30 days later. Tibia-patellar tendon-patella complexes were harvested and prepared for mechanical testing as previously described [4]. *Mechanical Testing*: Uniaxial, viscoelastic testing was performed with an Instron 5848. The testing protocol consisted of 10 cycles of preconditioning, followed by stress relaxations at 3%, 4%, and 5% strain. Following each stress relaxation, frequency sweeps of 10 cycles at 0.1, 1, 5, and 10Hz were performed. A ramp-to-failure followed the 5% stress relaxation. Percent relaxation, dynamic modulus (E*), and phase shift (δ) were quantified for each stress relaxation and frequency sweep. Stiffness, modulus, maximum load, and maximum stress were quantified from the ramp-to-failure data. *Statistics*: For all mechanical properties, one-way ANOVAs with Bonferroni post-hoc tests were used to compare across genotypes. Significance was set at $p \leq 0.05$, and trends were set at $p \leq 0.10$.

RESULTS: No differences in cross-sectional area (CSA) were observed between genotypes (data not shown). *Quasi-Static Mechanics*: *Col5a1*$^{-/-}$ (NULL) tendons had a decreased modulus relative to WT tendons (Fig 1). No differences in stiffness, max load, or max stress were observed between genotypes (data not shown). *Stress Relaxation*: *Col5a1*$^{+/-}$ (HET) tendons exhibited increased stress relaxation compared to WT tendons at 4% strain (Fig 2). NULL tendons trended towards increased stress relaxation compared to WT tendons at 4% strain. No differences were observed in stress relaxation between genotypes at 3% and 5% strain. *Dynamic Mechanics*: At 3% strain, NULL tendons had increased tan(δ) values compared to WT tendons at 0.1Hz (trend), 1Hz, and 5Hz and had increased tan(δ) values compared to HET tendons at 0.1Hz (data not shown). HET tendons had increased tan(δ) values compared to WT tendons at 1Hz and 5Hz (trend). At 4% strain, NULL tendons had increased tan(δ) values compared to WT tendons at all frequencies and trended towards higher tan(δ) values relative to HET tendons at 0.1Hz and 1Hz (Fig 3A). HET tendons had increased tan(δ) values compared to WT tendons at all frequencies (trend at 0.1Hz). At 5% strain, NULL tendons had increased tan(δ) values compared to WT tendons at all frequencies (Fig 3B). NULL tendons had increased tan(δ) values compared to HET tendons at 1Hz and 5Hz, with trending increases at 0.1Hz and 10Hz. No differences in dynamic moduli were observed between genotypes across strain levels and frequencies (data not shown).

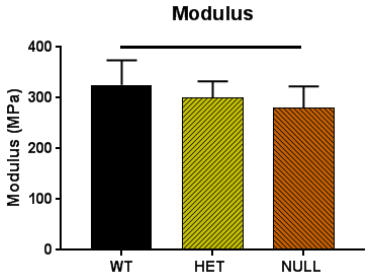

Fig 1. Elastic modulus. NULL tendons exhibited a decreased modulus relative to WT tendons. Solid bars indicate $p \leq 0.05$.

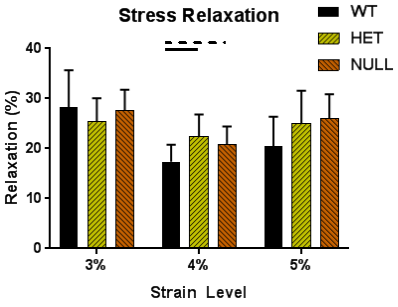

Fig 2. Stress relaxation. HET and NULL tendons displayed increased stress relaxation compared to WT tendons at 4% strain. Solid bars indicate $p \leq 0.05$, and dashed bars indicate $p \leq 0.1$.

DISCUSSION: Surprisingly, acute reduction in collagen V expression in mature tendons led to numerous changes in tendon viscoelastic properties. NULL tendons exhibited increased stress relaxation at 4% strain and increased tan(δ) values at nearly every strain and frequency. HET tendons exhibited increased stress relaxation at 4% strain and displayed intermediate tan(δ) values between those of WT and NULL tendons. These results are in direct contrast to our hypothesis, as knockdown of collagen V increased tendon viscoelasticity in an allele dosage-dependent manner. While mature tendons were generally believed to be quiescent tissues, there is growing evidence that tendon fibril networks are dynamic and remodel on shorter time scales than previously thought [5]. Results of this study strongly support the notion of these dynamic networks, with collagen V playing a large role in regulating fibril properties beyond the developmental time frame. While this study is limited by global knockout models and potential confounding effects on neighboring tissue, the induced and short period of knockdown minimizes these effects. Future studies will analyze the composition and gene expression of these collagen V-knockdown tendons to further elucidate the surprising regulatory role of collagen V in mature tendons. Overall, this study demonstrates that acute reduction of collagen V expression in mature tendons leads to an increase in their viscoelastic properties.

SIGNIFICANCE: This study reveals that acute reduction in collagen V expression increases viscoelasticity in mature tendons. These results provide further insight into the surprising role of collagen V in regulating mechanical properties during tendon homeostasis.

REFERENCES: [1] Symoens S et al. *Hum Mutat*. 2012. [2] Malfait F & De Paepe A. *AEMB*. 2014. [3] Sun M et al. *Am J Pathol*. 2015. [4] Dunkman AA et al. *Matrix Biol*. 2013. [5] Yeung CC & Kadler KE. *Curr Top Dev Biol*. 2019.

ACKNOWLEDGEMENTS: This work was supported by the NIH (R01AR065995, P30AR069619) and the NSF GRFP.

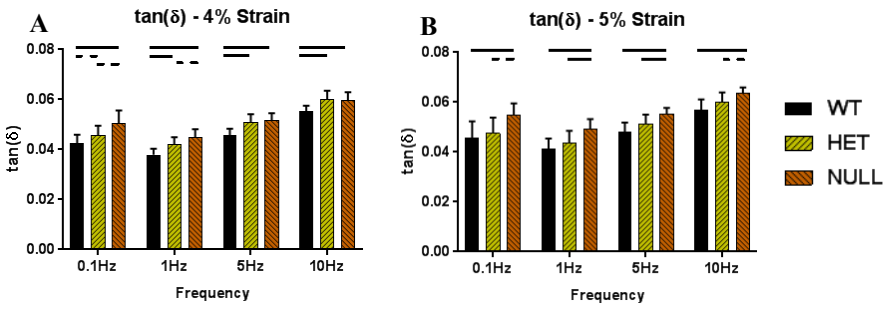

Fig 3. Phase shift. (A,B) NULL tendons had higher tan(δ) values than WT tendons at every frequency of both strains. HET tendons exhibited intermediate tan(δ) values between those of WT and NULL tendons. Solid bars indicate $p \leq 0.05$, and dashed bars indicate $p \leq 0.1$.

Microdialysis as a Longitudinal, *In Vivo* Assessment of Achilles Tendon Healing in a Rat Model

Joseph B. Newton, Snehal S. Shetye, Courtney A. Nuss, Matthew M. Counihan Daniel C. Farber, Louis J. Soslowsky
McKay Orthopaedic Research Laboratory, University of Pennsylvania, Philadelphia, PA

DISCLOSURES: Joseph B. Newton (N), Snehal S. Shetye (N), Courtney A. Nuss (N), Matthew M. Counihan (N), Daniel C. Farber (N), Louis J. Soslowsky (N).

Josebr@seas.upenn.edu

INTRODUCTION: The Achilles tendon is the most frequently ruptured tendon, leading to significant pain, loss of function, and healthcare costs [1]. *In vivo* assessment of healing after an Achilles tendon rupture can provide valuable metrics not only to monitor healing, but also to guide treatment options [2,3]. Specifically, *in vivo* assays such as ultrasound imaging, passive joint mobility assessments, and functional gait analysis can provide longitudinal measures of structural and functional properties of the healing tendon. However, these assays do not provide insight into the biologic changes in the healing tendon [4-6]. While microdialysis has been used to assess tendon healing in humans, it has not been used in an animal model of Achilles tendon injury [7,8]. Therefore, the objective of this study was to develop and pilot a novel use of microdialysis *in vivo* to directly measure key biologic markers of tendon healing and matrix deposition in the rat Achilles tendon. We hypothesized that, following Achilles injury, metabolite and procollagen concentrations would significantly increase indicating higher metabolic activity and collagen synthesis, respectively.

METHODS: *Experimental Design:* After facility acclimation, six, 4-month male Sprague Dawley rats underwent unilateral blunt transection of the right Achilles tendon without repair (IACUC approved). The right hind limb was immobilized for 7 days. Microdialysis measurements were taken before injury and 7, 14, and 21 days post injury. *Dialysate Collection and Analysis:* Under isofluorane anesthesia and ultrasound guidance, a microdialysis catheter (CMA 71; CMA Microdialysis AB; 100kDa molecular cutoff, 0.5mm outer diameter; 4mm in length) was introduced from the proximal aspect of the tendon towards the calcaneus. The active part of the membrane was placed in the rupture site and a perfusion fluid of artificial CSF with 3% 500kDa dextran (Sigma Aldrich) was used. The fluid was pumped through the inner tube of the catheter into the space between the inner tube and the semipermeable catheter membrane, where the exchange between the interstitial and perfusion fluid takes place. The resultant dialysate solution was transmitted from the catheter and collected in a 1.5mL vial (Microvial, CMA Microanalysis AV). With a perfusion speed of 1.0 µL/min, samples were collected for 2.5 hours. Due to fluid pump adjustment during the first few minutes, trauma from the probe insertion, and to remain conservative, the first 30 minutes of dialysate was discarded. Lactate, pyruvate, glucose, glutamate, glycerol, and procollagen type I N propeptide (PINP), concentrations were quantified via ELISAs. *Statistics*: All comparisons were made using the nonparametric Kruskal-Wallis ANOVA followed by Dunn's post hoc tests, which compared values at 7, 14, and 21 days post injury to preinjury values.

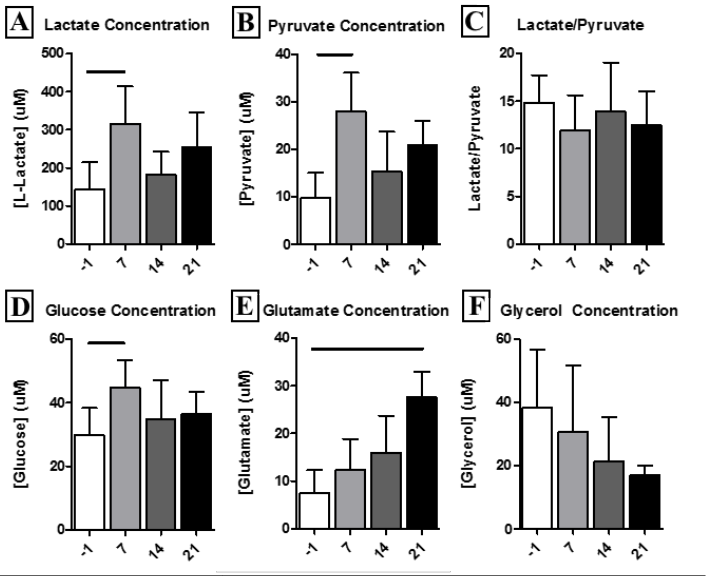

Figure 1. ELISA results from dialysate prior to injury (-1) and 7, 14, and 21 days post injury. Lactate (A) and pyruvate (B) concentrations peaked at 7 days post-injury while their relative ratio (C) was maintained. Glucose (D) peaked at day 7. Glutamate (E) was significantly increased at day 21. No changes were found in glycerol (F). Data as mean +/- standard deviations; bar indicates significance.

RESULTS: Lactate (Fig.1A) and pyruvate (Fig.1B) concentrations significantly increased 7 days post-injury, with no changes in lactate:pyruvate ratio at any time points (Fig.1C). Glucose concentration 7 days post-injury showed significant increases (Fig.1D). Glutamate was elevated 21 days following injury (Fig.1E). No changes were found in glycerol concentration following injury (Fig.1F). PINP concentrations were decreased at each post-injury time point compared to pre-injury measures (Fig.2).

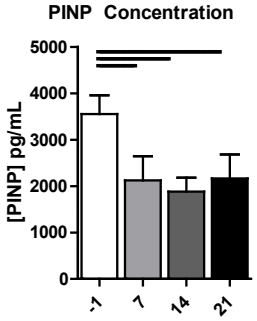

Figure 2. ELISA results showed a decrease in PINP concentration throughout healing compared to pre-injury levels. Data as mean +/- standard deviations; bar indicates significance.

DISCUSSION: Results indicate an early increase in overall metabolic activity and simultaneous decrease in collagen I production following Achilles injury. Increases in lactate and pyruvate 7 days post-injury indicate increased anaerobic and aerobic metabolic activity, respectively, as the resident cell population begins tissue repair. No changes in the lactate:pyruvate ratio demonstrate that the local environment is sufficiently oxygenated, as aerobic and anaerobic activity levels are maintained throughout healing [7]. Under normal healing conditions, angiogenesis peaks around day 7 in a healing tendon [9], which is supported by the early increase in glucose concentration. This increase in glucose concentration may also indicate increased metabolic activity immediately following injury, concurrent with the lactate and pyruvate changes shown. Glutamate concentration peaks at 21 days post-injury in congruence with nerve ingrowth [7]. Glycerol is a marker for cellular damage, and results show no changes in the metabolite's concentration, thus the severity of cellular damage remains unclear in our injury model [7,8]. PINP decreased immediately following injury, demonstrating a reduction in collagen I production. The study timeline was likely not long enough to see the expected increase in collagen I production as the tendon begins the remodeling phase of healing in which collagen III in the fibrotic scar tissue is replaced by more aligned collagen I [2]. Future studies will investigate changes in the biological environment of a healing Achilles tendon in response to exercise and new modalities to improve healing outcomes.

SIGNIFICANCE: This study demonstrates that microdialysis is a viable *in vivo*, longitudinal measure of Achilles tendon healing in a rat model. This technique will provide valuable metrics to monitor the biological environment in healing Achilles tendons.

REFERENCES: [1] Holm C et al., 2014. *Scand J Med Sci Sports*, 25:e1-10. [2] Auijla R et al., 2018. *Foot Ankle Surg*, 24:336-341. [3] Jandali Z et al., 2018. *J Reconstr Microsurg*, 34:632-641. [4] Riggin CN et al., 2019. *Ultrasound Med Biol*, 45:1841-1849. [5] Pardes A et al., 2016. *J Biomech*, 49:376-381. [6] Freedman BR et al., 2017. *J Biomech*, 56:55-60. [7] Greve K et al., 2012. *Scan J Med Sci Sports*, 22:e55-63. [8] Alim A et al., 2016. *BMJ Open Sport Exerc Med*, 2:e000114. [9] Gelberman R et al., 1991. *J Bone Joint Surg Am*, 73:868-881. [10] Neilsen M et al., 2013. *Am J Transl Res*, 5:303-315

ACKNOLEDGEMENTS: The authors acknowledge the contributions of the Dani Lab at the University of Pennsylvania, specifically Dr. William Doyon for his assistance with microdialysis. This study was supported by the Penn Center for Musculoskeletal Disorders (P30 AR069619) and the NIH (R01AR064216).

Liquid Poly-N-Acetyl Glucosamine (sNAG) Improves Achilles Tendon Healing in a Rat Model

Nuss CA[1], Huegel J[1], Finkielsztein S[2], Soslowsky LJ[1]
[1]McKay Orthopaedic Research Laboratory, Philadelphia, PA
[2]Marine Polymer Technologies, Inc., Burlington, MA

Disclosures: Nuss CA (N), Huegel J (N), Finkielsztein S (3A- Marine Polymer Technologies, Inc.), Soslowsky LJ (5)

Introduction: The Achilles tendon, while the strongest and largest tendon in the body, is frequently injured. Even after surgical repair, patients risk re-rupture and typically have long-term deficits in function, with a low rate of return to pre-injury levels of activity [1]. Various forms of biological augmentation have been utilized in an attempt to improve tendon repair [2]. Poly-N-acetyl glucosamine (sNAG) polymer has been shown to increase the rate of healing of venous leg ulcers, with an 86% success rate clinically [3]. Additionally, use of this material improved tendon-to-bone healing in a rat model of rotator cuff injury and repair [4]. However, whether this nanofiber material, in an injectable liquid formulation, could improve soft tissue tendon healing after Achilles injury is unknown. Therefore, the purpose of this study was to investigate the healing properties of sNAG containing membranes in a rat partial Achilles tear model. We hypothesized that sNAG would improve tendon healing as measured by improved mechanical properties and cellular morphology.

Methods: *Study Design*: 32 adult male Sprague-Dawley rats (400-450g) were used in this IACUC-approved study. All animals underwent a partial-width, full thickness injury using a 1.5 mm biopsy punch through the right Achilles tendon as described [5]. After injury, animals were randomized into two groups, receiving either 10 µl of 0.9% saline (control group) or 10 µl of 20 mg/ml sNAG polymer gel (sNAG group). Animals were allowed normal cage activity after surgery, without immobilization. Animals received repeat saline or sNAG injections at the site of the injury through the skin at one and two weeks post-surgery. All animals were sacrificed three weeks after injury. *Ex Vivo Assessments*: The Achilles-calcaneus complex was immediately harvested and processed for histological analysis including quantitative collagen fiber organization analysis (n=6/group). All other animals (n=10 per group per time point) were frozen at -20°C and later thawed for dissection and mechanical testing. For testing, the Achilles tendon and foot complex were dissected and the calcaneus was potted in poly(methyl methacrylate). While immersed in 37°C phosphate-buffered saline and in a physiologic orientation, the Achilles tendons were gripped and subjected to a mechanical loading protocol consisting of: preloading, stress relaxation at 6% strain, dynamic frequency sweeps, and fatigue cycling under load control until specimen failure. *Statistics:* Mechanical testing and collagen fiber organization data were evaluated using two-tailed t-tests after confirming data normality. Semi-quantitative histological comparisons were made using Mann-Whitney U tests. Significance was set at $p<0.05$ for all comparisons.

Results: *Mechanical properties*: At three weeks after injury, there was no difference in tendon cross-sectional area (not shown). Tendon stiffness was improved with sNAG treatment (Fig 1A), but modulus was not different between groups (Fig 1B). Frequency sweeps demonstrated an increase in dynamic modulus across tested frequencies (Fig 1C), but tanδ, a measure of force dissipation, was not different (not shown). Fatigue testing demonstrated increases in tendon secant stiffness (Fig. 1D) and tangent stiffness (Fig. 1E) throughout fatigue life for sNAG-treated tendons compared to controls. There was no difference in cycles to failure (Fig. 1F), or other properties measured (not shown). *Histologic observations*: Semi-quantitative grading did not demonstrate differences in cell density (Fig. 2A) or cell shape (Fig. 2B) at the injury region. Collagen alignment in this region was also not different between groups (Fig. 2C). Representative images of the injury region for both groups are shown in Figure 2D.

Discussion: This study investigated the effects of repeated sNAG polymer application on tendon healing after partial Achilles injury. Although several parameters did not exhibit differences between treatment groups, other results demonstrate that sNAG has a positive effect on rat Achilles tendon healing at three weeks after a full thickness, partial width injury. Quasistatic testing demonstrated increased tendon stiffness with sNAG treatment, which continued during fatigue cycling, as shown in increased tangent and secant stiffness across fatigue life. Increased dynamic modulus also suggests improved viscoelastic properties with sNAG treatment. Importantly, use of this material did not have any negative effects on any measured parameter. Previous studies suggest that this material may mitigate pain after rotator cuff injury [4]. Functional testing such as gait assessment might be valuable, potentially expanding the use of this material as a less invasive treatment for painful Achilles tendonitis [6]. Additionally, dosage studies and number of repeated sNAG injections may optimize the use of sNAG for soft tissue tendon healing. Finally, studies to elucidate the mechanism of action for the changes identified are important.

Significance: Repeated injections of sNAG polymer improve Achilles tendon properties after partial tear. These results support further study of this material as a minimally invasive treatment modality for tendon healing.

References: [1] Barfod KW et al. J Bone Joint Surg, 2014. [2] Shapiro E et al. Curr Rev Musculoskelet Med, 2015. [3] Kelechi, TJ et al. J Am Acad Derm, 2011. [4] Nuss CA et al. Ann Biomed Eng, 2017. [5] Huegel J et al. J Biomech, 2019. [6] Barg A & Ludwig T. Foot Ankle Clin, 2019.

Acknowledgements: We thank Stephanie Weiss and Peter Chan for assistance.

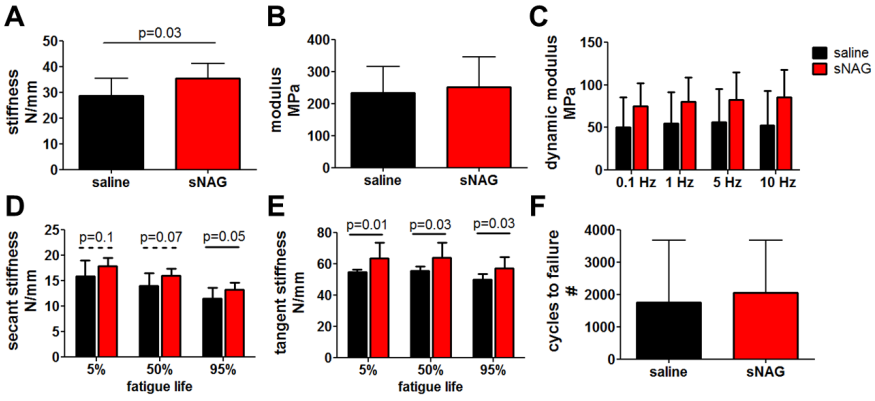

Figure 1. **Mechanical Properties.** Three weeks after injury, sNAG treated tendons had (A) increased stiffness, (B) no change in modulus, (C) increased dynamic modulus across testing frequencies, (D) increased secant stiffness, and (E) increased tangent stiffness. There were no changes in (F) cycles to failure between groups. Data shown as mean+SD.

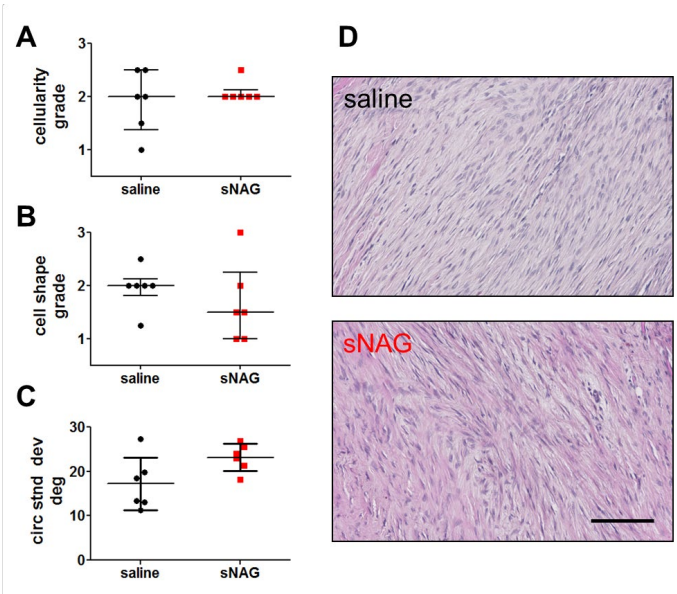

Figure 2. **Histological Properties.** There were no differences between groups for (A) cellularity, (B) cell shape, or (C) collagen alignment. Representative images of the injury region are shown in (D). Data represented as median±IQR in A and B, and as mean±SD in C. Scale bar in D: 100 µm.

Structural and Cellular Responses of Supraspinatus Tendon Enthesis and Subchondral Bone to Pregnancy, Lactation, and Post-Weaning Recovery

Yilu Zhou, Yihan Li, Zachary Davis, Wenzheng Wang, Ashley K. Fung, Snehal S. Shetye, Xi Jiang, Andrew F. Kuntz, Nathaniel Dyment, Louis J. Soslowsky, X. Sherry Liu

Department of Orthopaedic Surgery, University of Pennsylvania, Philadelphia, PA, USA. yiluz@pennmedicine.upenn.edu

Disclosures: All authors have nothing to disclose.

INTRODUCTION: The maternal skeleton undergoes dramatic bone loss during pregnancy and lactation [1], and fluctuating hormone levels increase the risk of musculoskeletal joint disorders such as shoulder pain [2-3]. Previously, we discovered transient changes in mechanical properties of the supraspinatus tendon during pregnancy [4]. However, the cellular mechanisms behind such effects in a reproductive cycle remain unknown. Since, the supraspinatus tendon transfers force from the muscle to the bone of the humerus through the enthesis, the objective of this study was to track the structural and cellular responses in specific regions of the supraspinatus tendon enthesis and underlying humeral bone. We hypothesized that differential effects of pregnancy, lactation, and post-weaning on cellular activities would alter the dynamic change of microstructure in the enthesis and subchondral bone.

METHODS: (IACUC approved) *In vivo μCT study*: Thirteen female SD rats (7 virgins and 6 rats with a complete reproductive cycle) received *in vivo* μCT scans of the right proximal humeri at mating (baseline), end of 3-week pregnancy, 3-week lactation, and 6-week post-weaning recovery using VivaCT 80 (Scanco Medical AG, voxel size 21μm). The humerus was divided into 3 regions of interests (3 ROI: the region below supraspinatus tendon enthesis, the epiphysis, and the metaphysis, Fig 1A) and each region was subjected to trabecular bone microstructure analysis. *Histomorphometry Study*: Twenty-four rats (aged 7 month at euthanasia) were assigned to 4 groups (n=6/group): virgin, pregnancy (euthanized at parturition), lactation (euthanized after 2-week lactation), and recovery group (euthanized 2-week post weaning). All rats were injected with calcein green, alizarin red, and tetracycline at 16, 9, 2 days before euthanasia. The left shoulder was harvested and cryo-embedded. Cryo-sections were first imaged to identify fluorochrome mineralization labels, followed by tartrate-resistant acid phosphatase (TRAP) staining to visualize catabolic enzyme activities; and a subsequent toluidine blue staining for identifying cell population and different zones in the tendon enthesis site: unmineralized fibrocartilage (UF), tidemark (TM), mineralized fibrocartilage (MF), and bone (B). *Statistics*: Longitudinal comparisons were made using 2-way, repeated-measures ANOVA with baseline adjustment and Bonferroni corrections for post hoc tests. All cross-sectional comparisons were made using 1-way ANOVA and Tukey's HSD for post hoc tests.

RESULTS: All differences and changes reported here are statistically significant ($p<0.05$). Across a reproductive cycle, similar changes were seen in trabecular bone microstructure at the epiphysis (data not shown) and the region adjacent to the enthesis (Fig 1D-F), with the changes being more striking at the latter (data not shown). Specifically, at the enthesis region, no change in bone microstructure was observed during pregnancy. In contrast, lactation resulted in 41%, 12%, and 7% reduction in BV/TV, Tb.N, and Tb.Th, respectively (Fig 1B, D-F). Weaning triggered a substantial anabolic response (Fig 1C), resulting in complete recovery in Tb.N and Tb.Th, and greater BV/TV in post-weaning rats than virgins (Fig 1D-F). Different from the epiphysis and enthesis region, the metaphsysis underwent greater bone loss during pregnancy. By the end of lactation, there were 69%, 42%, and 18% decreases in BV/TV, Tb.N, and Tb.Th than baseline, respectively (Fig 1G-I). Even 6 weeks after weaning, Tb.N still remained 25% lower than the baseline (Fig 1H). Histomorphometry images showed TRAP activities on bone surface in all groups and the expression level reached the peak during lactation (Fig 2A-F). Furthermore, the fraction of TRAP-expressing osteocytes (Fig 2G) in bone at the base of the enthesis rapidly increased from 8% (baseline) to 30% (lactation). Multicolor mineralizing labels were found in the subchondral bone near the enthesis in all groups, with the strongest activities observed in the recovery group (Fig 2D), which was consistent with μCT data showing substantial trabecular bone recovery after weaning. However, flurochrome labels at the enthesis tidemark were only found in the pregnancy group (Fig 2B&E). Within the mineralized zones of the enthesis, we found that bone fraction (Fig 2H) and osteocyte/fibrochondrocyte number ratio (Fig 2I) in recovery group were 21% and 40% greater than that of lactation group, respectively.

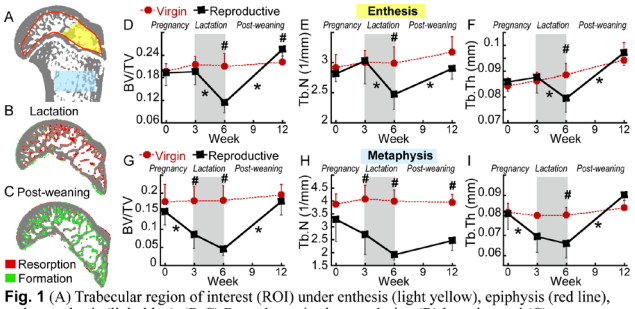

Fig. 1 (A) Trabecular region of interest (ROI) under enthesis (light yellow), epiphysis (red line), and metaphysis (light blue). (B-C) Bone dynamic changes during (B) lactation and (C) post-weaning recovery. Red indicates bone resorption and Green indicates bone formation. (D-I) Changes of trabecular bone microstructure at the (D-F) enthesis and (G-I) metaphysis. $p<0.05$: # Virgin ≠ Reproductive; * difference between two time points in Reproductive group.

DISCUSSION: Pregnancy, lactation, and weaning cause substantial fluctuations and complex interactions of circulating calciotropic and sex hormones. These changes result in upregulated TRAP expression in both osteoclasts and osteocytes during lactation and subsequent increases in bone formation adjacent to the enthesis. In the humeral epiphysis, substantial bone loss was observed during lactation followed by a complete recovery after weaning, unlike the metaphysis which did not fully recover. Moreover, striking changes were perceived specifically at the location adjacent to enthesis, where tensile force from tendon is transmitted to underlying bone. In contrast to the metaphysis, the epiphysis and the location adjacent to enthesis are resistant to pregnancy-induced bone loss. Interestingly, we found an activation of mineral deposition from enthesis fibrochondrocytes at the tidemark (Fig 2E) during pregnancy, but did not detect structural changes in the enthesis fibrocartilage. Furthermore, tidemark mineral deposition was also observed in pseudopregnancy rats (data not shown), potentially due to fibrochondrocytes activated by elevated progesterone level during pregnancy and pseudopregnancy [5]. Our results also demonstrated osteocyte peri-lacunar/canalicular remodeling (PLR) [6] at the subchondral bone during lactation. Future studies are required to gain more insights into the regulatory role of osteocyte PLR in balancing calcium homeostasis and tissue mechano-sensitivity at the tendon enthesis.

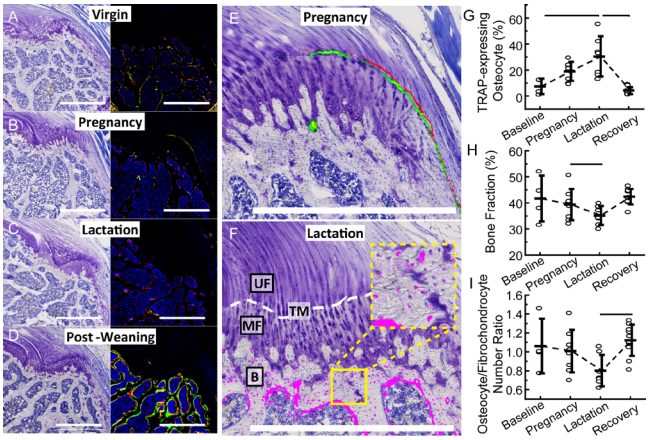

Fig. 2 (A-D) Representative cryo-images from (A) Virgin, (B) Pregnancy, (C) Lactation, and (D) Post-weaning group. White bar =1mm. Left: toluidine blue staining; Right: fluorescent images; Green, Red, Yellow indicate flurochrome mineralizing labels; blue: nucleus; pink: TRAP staining. (E) A representative Toluidine blue image overlapped with flurochrome mineralizing labels from Pregnancy group. (F) Representative Toluidine blue image overlapped with TRAP staining (pink) from Lactation group. Tendon enthesis zones: unmineralized fibrocartilage (UF),tidemark (TM), mineralized fibrocartilage (MF), and bone (B). (G-I) Quantifications in mineralizd enthesis:(G) TRAP expressing fraction of osteocyte, (H) bone fraction, (I) osteocyte/fibrochondrocyte ratio. Solid line indicates $p<0.05$ between two groups.

SIGNIFICANCE: This study demonstrated that the adaptive responses in cellular activities during female reproduction optimize the balance between calcium homeostasis and the structural and mechanical integrity of tendon enthesis and underlying bone.

REFERENCES: [1] Kovacs, *Physiol Rev.,* 2015; [2] Watt *et al., Post Reprod Health*, 2018; [3] Cucchi *et al., Joints*, 2017; [4] Fung *et al., SB3C,* 2019; [5] Bowman *et al., JBMR*, 1996; [6] Qing *et al*., *JBMR*, 2012.

ACKNOWLEDGEMENTS: NIH/NIAMS R01-AR071718, NSF #1653216, and Penn Center for Musculoskeletal Disorders (P30-AR069619).